NBSIR 78-1511

EXPERIMENTAL AND THEORETICAL ANALYSIS OF QUASI-STEADY SMALL-SCALE ENCLOSURE FIRES

J. G. Quintiere, B. J. McCaffrey and K. DenBraven

Center for Fire Research
National Engineering Laboratory
National Bureau of Standards
Washington, D.C. 20234

October 1978

U.S. DEPARTMENT OF COMMERCE, Juanita M. Kreps, *Secretary*
Dr. Sidney Harman, *Under Secretary*
Jordan J. Baruch, *Assistant Secretary for Science and Technology*
NATIONAL BUREAU OF STANDARDS, Ernest Ambler, *Director*

NBSIR 78-1511

EXPERIMENTAL AND THEORETICAL ANALYSIS OF QUASI-STEADY SMALL-SCALE ENCLOSURE FIRES

J. G. Quintiere, B. J. McCaffrey and K. DenBraven

Center for Fire Research
National Engineering Laboratory
National Bureau of Standards
Washington, D.C. 20234

October 1978

U.S. DEPARTMENT OF COMMERCE, Juanita M. Kreps, *Secretary*

Dr. Sidney Harman, *Under Secretary*

Jordan J. Baruch, *Assistant Secretary for Science and Technology*

NATIONAL BUREAU OF STANDARDS, Ernest Ambler, *Director*

CONTENTS

LIST OF FIGURES

LIST OF TABLES

TABLE OF NOMENCLATURE

A	Surface area
c	Orifice coefficient
C, C_g	Specific heat of solid, fluid
F_{dF}	Geometric configuration factor between the thermal discontinuity plane and the floor
F_{FS}	Geometric configuration factor between the lower walls and fuel surface
g	Gravitational acceleration
h	Convective or total heat transfer coefficient
H	Height
ΔH	Heat of combustion
ΔH_v	Heat of volatilization
k	Thermal conductivity
k_e	Entrainment constant
k_g, k_{soot}	Absorption coefficients for gases, and soot
K	Thermal conductance
L	Length of room
$\dot{m}$	Rate of mass flow
p	Pressure
$\dot{q}$	Rate of heat flow
r	Mass air to fuel ratio
T	Temperature
W	Width of room
X_n	Height of neutral plane
X_d	Height of thermal discontinuity
β	Parameter defined by eq. 6
γ	Area ratio, A_F/A_W
δ	Wall thickness
ε	Emissivity
ρ	Density
ω	Parameter defined by eq. 7

Subscripts

a	Air
b	Burning
d	Thermal discontinuity
e	Entrainment
f	Flame
fuel	Fuel
F	Floor
g	Hot gaseous combustion products
n	Neutral plane
o	Doorway
p	Plume
py	Pyrolysis
r	Radiation
s	Fuel surface
v	Volatilization
w	Hot walls and ceiling

Superscript

()"	Per unit area

EXPERIMENTAL AND THEORETICAL ANALYSIS OF QUASI-STEADY SMALL-SCALE ENCLOSURE FIRES

J. G. Quintiere, B. J. McCaffrey and K. DenBraven

Abstract

Forty-six small-scale experiments were conducted to measure the characteristics of horizontal plastic (PMMA) pool fires in an enclosure as a function of doorway width and fuel area. A 0.30 m high enclosure was instrumented to measure sample mass loss, the upper gas layer and ceiling temperatures, heat flux to the floor, and the pressure drop across the doorway. Results are reported for the maximum steady burning period; however, a few cases do not seem to have reached a steady state. For small sample sizes, a distinct fire plume could be perceived in the enclosure, while for larger sample sizes flames tended to fill the enclosure (sometimes to within 2 or 3 cm of the floor), and extended out the door opening.

The rate of mass loss is a strong function of the radiative feedback from the enclosure. However, reduced oxygen concentration in the flow entrained by the fire plume seems also to affect the mass loss rate. For the smaller doorway widths, the rate of mass loss increases almost directly with ventilation. As the width is increased, the mass loss rate instead becomes a function of sample area and radiative heat transfer. For some sample sizes, as the doorway width is increased a maximum rate of mass loss is achieved, followed by a decrease in burning rate at higher ventilation levels. The temperatures and floor heat flux also tend to follow this trend.

The data were then compared to the results of a theoretical model. Agreement between theory and data is qualitatively good. But overall, good quantitative agreement is not achieved. This lack of agreement appears consistent with inaccuracies of the flame radiation model and an incomplete description of the flame chemistry.

Key words: Burning rate; enclosure fires; experiment; mathematical models; radiation; small scale; ventilation.

1. INTRODUCTION

One basic objective of fire safety research is the evaluation of the risk of fire growth within a room. Such an evaluation must consider all possible fuel sources and their arrangement, as well as the geometry and description of the enclosure. The present study is directed at improving the methodology for making this evaluation.

Specifically, a global mathematical model has been formulated [1][1] for an idealized mode of fire growth. It considers the fire as a steady burning horizontal slab of fuel on the floor of the compartment. The resulting fuel vaporization and corresponding thermal and flow characteristics are then calculated. In general, the model can be used to predict thermal conditions which may be judged as conducive to rapid fire growth and spread. In order to validate the model, experiments have been conducted on a small scale to match this idealized mode of burning. This paper reports on the comparison of that data with the theoretical results.

Traditionally, compartment fire research has been aimed at the fully-developed fire with application primarily to the prediction of the fire resistance of structural members. This work has been done essentially with wood cribs, and has elucidated two burning regimes: "fuel controlled" in which the pyrolysis rate is dependent on the exposed fuel surface area, and "ventilation controlled" in which the pyrolysis rate is dependent on the size of the compartment opening (or more precisely the factor $A_o\sqrt{H_o}$). The latter regime has not yet been quantitatively explained, although it is generally accepted that a reduction in airflow seems to reduce the extent and rate of heat transfer to the fuel surface, thereby reducing and controlling the pyrolysis rate. The work of Gross and Robertson [2] illustrates these two regimes of compartment burning, while more recently the work of Thomas and Nilsson [3] illustrates a third burning regime related to the porosity of the cribs.

To study developing fires in rooms, many have considered flat horizontal or vertical slabs of fuel. These surfaces exhibit a greater sensitivity to radiation from the enclosure, resulting in a greater pyrolysis rate than for crib fires in rooms. For example, Friedman [4] cites an increase in the rate of mass loss for a wood crib fire in a room of up to 1.6 times its corresponding free burn value, yet a threefold increase was associated with

---
[1] Numbers in brackets refer to references listed at the end of this paper.

the burning of a horizontal slab of polymethyl methacrylate (PMMA). Experiments with liquid fuel pool fires in compartments [5,6] indicate a similar relationship between mass loss rate and $A_o\sqrt{H_o}$ as seen in wood crib fires, but with less enhancement of burning as that found for PMMA.

In recent years the mathematical modeling of developing fires has received increasing attention. This has occurred because of the need to evaluate furnishings items and materials in a room fire scenario, and ultimately to predict the spread of the fire through a building. Representative of the current state of modeling are an analysis by Tanaka [7] of fire spread over the interior surfaces of a room, and a generalized computer code developed by Emmons et al. [8]. This code has favorably predicted transient measurements from full-scale experimental room fires. In contrast, the model to be presented here does not consider time as a parameter. Instead, it can be used to indicate the "critical" values of fuel area and room opening at which thermal conditions in the room would exceed a tolerable level or would promote further fire growth.

2. DESCRIPTION OF THE EXPERIMENT

Square slabs of polymethyl methacrylate (PMMA) were burned in a small compartment constructed of low density alumina silica block. A sketch of the experimental arrangement is shown in figure 1. The internal dimensions of the enclosure were 0.30 m x 0.30 m x 0.56 m deep with a doorway height of 0.225 m and widths ranging from 0.015 m to 0.285 m. Five PMMA sample sizes were burned, ranging in face area from 0.0025 m^2 to 0.0225 m^2 with a constant thickness of 0.013 m. The PMMA was burned on a platform 0.03 m above the floor and centered 0.40 m from the doorway. The weight was continuously recorded by a (linear variable differential transformer type) load cell which supported the platform, and was sufficiently below the floor to remain cool. Two bare chromel-alumel thermocouples of 0.025 mm diameter wire were used to measure the upper gas and ceiling temperatures at the locations shown in figure 1. The ceiling thermocouple was pressed flush into the surface. A water-cooled thermopile heat flux sensor of absorptivity 0.97 was used to record the incident heat flux to the floor. The pressure difference across the compartment wall was measured with a sensitive electronic manometer.

Except in the flame region, the thermocouples yielded representative temperatures of the upper hot gas layer and upper walls and ceiling. The heat flux sensor indicated the incident radiative flux from the enclosure to the PMMA surface, since the PMMA flame has a small emissivity. The pressure drop measurement was used to estimate the induced flow rate through the doorway.

Forty-six experiments were conducted with the fuel size and doorway width varied. Runs were repeated if instruments malfunctioned or to check reproducibility; in general, reproducibility of the results was very good. The procedure for each experiment consisted of first inspecting and cleaning the probes. A mixture of PMMA chips and paraffin oil was used as an accelerant to insure uniform ignition of the PMMA sheet. The PMMA sample was lined along the sides and bottom with aluminum foil to prevent uneven burning at the edges. Just prior to ignition, a small amount of pentane was added to the PMMA surface. The sample was ignited and allowed to burn completely, during which time the data were recorded continuously.

For the most part, two modes of burning could be discerned in these experiments. The first mode was exhibited by the smaller PMMA samples. This was characterized by a distinct pulsating laminar-like flame plume within the enclosure. These samples burned slowly, with complete consumption generally taking 25 to 30 minutes. A steady burning period persisted for a minimum of five minutes. The second mode of burning was exhibited by the larger size samples. The consumption period for this mode averaged about 15 minutes. These samples initially burned slowly and steadily, then the burning increased rapidly as turbulent flames stretched across the ceiling and extended out of the doorway. For the small door widths the flames filled the enclosure to within 2 to 3 cm of the floor. In general, a steady burning period could be discerned over the last several minutes of the burn, but in a few cases no steady-maximum burning was achieved before consumption (see appendix A).

3. EXPERIMENTAL RESULTS

The data were analyzed to determine the period of maximum steady burning and the corresponding average values of the variables measured. This was done by identifying a significant period over which the rate of mass loss was at its steady peak. The corresponding periods of maximum-steady temperature were nearly coincidental. These maximum-steady values are listed in table 1 along with their deviation during this "period of steady burning."

Also listed in table 1 are calculated values of induced airflow rate. This was determined using the following assumptions:

1. the fluid in the room is stratified into two horizontal regions of uniform temperature,
2. the pressure in the enclosure follows a hydrostatic distribution, and
3. an orifice flow model applies at the doorway.

The first assumption is generally acceptable, the second is valid based on the work of McCaffrey and Rockett [9], and Prahl and Emmons [10] have demonstrated the applicability of the third assumption. Based on these studies the procedure for calculating the induced airflow rate, $\dot{m}_a$ is as follows:

(neutral plane height i.e., the position of zero pressure drop and velocity in the doorway)

$$X_n = H - \frac{\Delta p}{\rho_a \left(1 - \frac{T_a}{T_g}\right) g} \qquad (1)$$

where Δp is the pressure difference at the ceiling height, H.
(exit mass flow rate)

$$\dot{m}_g = \frac{2}{3} c \, W_o \, \rho_a \sqrt{2g \left(\frac{T_a}{T_g}\right) \left(1 - \frac{T_a}{T_g}\right)} \left(H_o - X_n\right)^{3/2} \qquad (2)$$

(inlet air mass flow rate)

$$\dot{m}_a = \dot{m}_g - \dot{m}_v \qquad (3)$$

(Since numerous symbols will be used in the text, most will be defined in the table of nomenclature only.) The measured values of Δp, T_g, and $\dot{m}_v$ were used to determine X_n, $\dot{m}_g$, and $\dot{m}_a$. The flow coefficient, c, was taken as 0.7, but could be higher for this scale experiment [10]. In cases where the measured value of the pressure difference, Δp, was low due to soot clogging the pressure tap, values of airflow were not calculated. The application of this procedure could overestimate X_n by about 30% [9]. Since the flow coefficient for the exit can exceed 0.7 (but is not likely to be greater than 1), the net effect of variations in c and X_n could yield an estimated 20% error or less in $\dot{m}_a$.

4. THEORETICAL MODEL

The basis of the theoretical model has been previously derived [1]. Consequently, no detailed derivation will be presented; however, the equations will be listed along with a description of their significance. Basically the equations have been derived by applying the conservation laws to distinct spatial regions (or control volumes, CV) that possess an approximately uniform character. These regions are identified in figure 2. The fuel (CV_I) is considered to be a steadily vaporizing solid. The fire plume (CV_{II}) is considered to be the region in which all of the combustion occurs, and is assumed to be a cylinder for radiation calculations. The upper region (CV_{III}), roughly considered as the smoke layer, is considered to be at a uniform temperature, T_g. Energy balances are also applied to the upper walls and ceiling, and to the floor, to determine these surface temperatures. These surfaces are considered to be black for radiation calculations. The philosophy of this development has been to include all of the processes that have been identified and that are amenable to mathematical description. Chemical processes have not been completely modeled, and some processes have been modeled approximately since a more elaborate description may not be justified at this time.

4.1. Flow Model

The calculation to determine the rate of induced flow is based on Rockett's derivation [11]. The flow exiting the doorway has already been given by eq. (2). The airflow entering the compartment is given by:

$$\dot{m}_a = \frac{2}{3} c \, W_o \, \rho_a \sqrt{2g\left(1-\frac{T_a}{T_g}\right)} \left(X_n - X_d\right)^{1/2} \left(X_n + \frac{X_d}{2}\right). \qquad (4)$$

This same flow is assumed to be entrained in the fire plume and eq. (4) is based on the result from Steward [12] for a turbulent diffusion flame.

$$\dot{m}_a = \left(\frac{\rho_a}{\rho_v}\right) \omega \, \dot{m}_v \left[(\beta X_d + 1)^{5/2} - 1\right] \simeq \left(\frac{\rho_a}{\rho_v}\right) \omega \, \dot{m}_v \, (\beta X_d + 1)^{5/2} \qquad (5)$$

where

$$\beta = \frac{4}{5}(1-\omega)\left(\frac{5\pi^2 g \rho_v^{\,2} k_e^{\,4}}{12\, \dot{m}_v^{\,2}\, \omega^3}\right)^{1/5} \qquad (6)$$

and
$$\omega = \frac{1}{1 + \frac{\Delta H}{r C_g T_a}} \quad . \tag{7}$$

The applicability of this turbulent plume model may be questioned for this scale experiment since the flame did not always appear to be fully turbulent. Moreover, such models may not be very accurate near the base of the plume. In this regard, McCaffrey and Rockett [9] have found that the measured doorway airflow has a much stronger dependence on the fuel supply, $\dot{m}_v$, than eq. (5) indicates; and that the entrainment coefficient, k_e, appears to vary accordingly. Consequently an expression for k_e has been developed from the experimental results of $\dot{m}_a$ for large doorway openings. This was estimated as

$$k_e = 0.1 + 0.5\, \dot{m}_v \tag{8}$$

where $\dot{m}_v$ is in g/s.

Equations (3), (4), and (5) may be considered as having three unknowns: airflow rate, $\dot{m}_a$, neutral plane height, X_n, and the height of the hot layer, X_d. In fact, these were solved in that fashion with $\dot{m}_v$ specified and T_g determined through an iterative process from a solution of the energy equations to follow.

4.2. Energy Conservation for the Fuel (CV_I)

The solid is assumed to vaporize at a constant surface temperature, T_s, and steady burning is assumed. The vaporization rate, $\dot{m}_v$, for a solid of surface area, A_v, exposed to a net surface heat flux, $\dot{q}_s''$ is

$$\dot{m}_v = \frac{\dot{q}_s'' \; A_v}{C_{fuel}(T_s - T_a) + \Delta H_v} \quad . \tag{9}$$

The surface heat flux cannot easily be determined without a complete understanding of the flame chemistry and radiation properties. An approximate expression is used which at least includes the major contributing factors.

$$\begin{aligned} \dot{q}_s'' = {} & h_s(T_f - T_s) + \varepsilon_f \sigma T_f^4 + (1-\varepsilon_f) F_{dF} \sigma \left(\varepsilon_g T_g^4 + (1-\varepsilon_g) T_w^4\right) \\ & + (1-\varepsilon_f) F_{FS} \sigma T_F^4 - \sigma T_s^4 \end{aligned} \tag{10}$$

This sum represents the convective heat flux from the flame; the incident radiative flux from the flame, upper hot layer and surfaces, and the lower heated surfaces; minus the surface reradiation. The unsatisfactory aspects of this formulation may be obvious:

1. The flame temperature is constant and uniform over a prescribed volume.
2. The convective contribution ignores the effect of fuel vaporization and the convective coefficient has been treated as a constant, independent of the fuel dimensions.
3. Flame emissivity is based only on flame height, and is represented as

$$\varepsilon_f = 1 - \exp(-k_f H_f) \tag{11}$$

where

$$H_f = 16.2 \left[\frac{(r+\omega\rho_a/\rho_v)^2 \omega}{\rho_a^{\,2} g(1-\omega)^5} \right]^{1/5} \cdot \dot{m}_b^{\,2/5} \tag{12a}$$

or

$$H_f = X_d, \tag{12b}$$

whichever is smaller [12]. A representation that includes flame diameter, or flame shape in the compartment (if this were available), could improve this formulation.

4. The contributions of compartment radiation are based on approximate expressions for the interchange factors between these sources of radiation and the fuel surface. The geometric shape factor F_{dF} is calculated for parallel surfaces at the layer depth and the floor, and the shape factor between the lower walls and fuel surface is heuristically represented as

$$F_{FS} = 1 - \frac{W}{\sqrt{W^2 + 4X_d^{\,2}}} \quad . \tag{13}$$

4.3. Energy Conservation for the Fire Plume (CV_{II})

The assumptions for the energy balance on the fire plume are that all combustion occurs within that region, the fluid crosses into the hot layer region with temperature T_p, and the flame plume radiates as a cylinder at temperature T_f. Essentially, this energy balance equates the sum of the combustion energy and the radiant energy absorbed by the flame minus the energy radiated from the flame to the convected energy transported through the control volume (CV_{II}).

$$\dot{m}_b \Delta H + \varepsilon_f F_{dF} \sigma \left(\varepsilon_g T_g^4 + (1-\varepsilon_g) T_w^4\right) A_v - \varepsilon_f \sigma T_f^4 \cdot 2H_f \sqrt{\pi A_v}$$

$$= \dot{m}_g C_g (T_p - T_a) + \dot{m}_{py} \left[\Delta H_v + C_{fuel}(T_s - T_a) - C_g (T_s - T_a)\right] \tag{14}$$

Where there is insufficient air for complete combustion, $\dot{m}_a/\dot{m}_v < r$:

$$\dot{m}_b = \dot{m}_a/r, \tag{15a}$$

$$\dot{m}_{py} = \dot{m}_v - \dot{m}_b; \tag{15b}$$

and, for excess air, $\dot{m}_a/\dot{m}_v > r$:

$$\dot{m}_b = \dot{m}_v , \tag{16a}$$

and

$$\dot{m}_{py} = 0 . \tag{16b}$$

4.4. Energy Conservation of the Hot Upper Layer (CV_{III})

This energy balance considers only convective and radiative phenomena. It considers a uniform fluid temperature, T_g, and a uniform surface temperature, T_w, for the bounding walls and ceiling. These assumptions are good since this region is well mixed unless extensive combustion occurs within it. No mixing with the layer below is considered except for the plume penetration. This is not valid near openings where the entering air jet will entrain some hot fluid into it. This point will be addressed later.

$$\dot{m}_g C_g (T_p - T_g) = h_w A_w (T_g - T_w) + \dot{q}''_{r,w} A_w + \dot{q}''_{r,d} A_F + \sigma T_w^4 A_o \tag{17}$$

The net radiation from the gas to the walls is

$$\dot{q}''_{r,w} = \varepsilon_g \sigma T_g^4 + \gamma (1-\varepsilon_g) \sigma T_F^4 - \left[1-(1-\gamma)(1-\varepsilon_g)\right] \sigma T_w^4 \tag{18}$$

where

$$\gamma = A_F/A_w, \tag{19}$$

the ratio of floor to the wall and ceiling area bounding CV_{III}. The net radiative flux from the lower plane of the hot layer is

$$\dot{q}''_{r,d} = \varepsilon_g \sigma T_g^4 + (1-\varepsilon_g) \sigma T_w^4 - \sigma T_F^4 \tag{20}$$

The radiation emitted through the doorway is relatively small. Hence, it has been approximated in eq. (17). The emissivity of the hot upper layer is represented as a function of the soot concentration and the H_2O and CO_2 composition of the layer.

$$\varepsilon_g = 1 - \exp\left[(k_g + k_{soot})\ (H-X_d)\right] \tag{21}$$

where k_g and k_{soot} are the absorption coefficients for the gases and soot respectively.

4.5. Conservation of Energy for Upper Walls and Ceiling

Since the characteristic time for thermal penetration of the compartment walls was approximately 10 minutes, and most experiments exceeded this time, steady conduction was assumed for the enclosure structure. The resulting energy equation is

$$\dot{q}''_{r,w} + h_w\ (T_g - T_w) = K_w (T_w - T_a) \tag{22}$$

where $$K_w = \frac{1}{\frac{\delta}{k_w} + \frac{1}{h_a}} \tag{23}$$

which accounts for conduction through the wall and a convection loss on the outside.

4.6. Conservation of Energy for the Floor

A balance of radiation, convection, and conduction for the floor yields

$$F_{dF}\ \dot{q}''_{r,d} = h_F (T_F - T_a) + K_w (T_F - T_a). \tag{24}$$

4.7. Solution of the Conservation Equations

The algebraic equations were solved numerically employing a Newton-Raphson technique for first the flow equations (2) - (5), then the energy equations. Basically the procedure is to specify $\dot{m}_v$, and guess T_g to solve the flow equations for X_d, X_n, and $\dot{m}_a$. The energy equations are then solved for T_w, T_g, T_F, and A_v. This process is reiterated using a new value of T_g until satisfactory convergence is achieved (appendices D and E).

The values selected for the parameters that best matched the experimental conditions are listed in table 2. Some remarks explaining or justifying their selection are listed there also.

5. DISCUSSION OF RESULTS

The experimental results display a strong coupling effect between the rate of burning and the energy feedback to the fuel from the compartment. The theoretical results are in good qualitative agreement with the data, and in some cases, good quantitative agreement also. These features are evident in figures 3-5 where the rate of mass loss, gas temperature, and radiative heat flux to the floor have been plotted against fuel surface area for each of the experimental doorway widths (W_o) selected. The ceiling temperature results have not been plotted since they are similar in character to the gas temperature results for theory and experiment.

Figure 3a shows that as the fuel area is increased, the rate of mass loss increases, almost linearly with A_v at first, then more rapidly as the compartment is heated and significant radiation is received by the fuel. Eventually so much fuel is vaporized that it cannot be burned within the compartment due to insufficient air. This excess fuel serves to dilute the products of combustion and hence to reduce the temperature and rate of heat flux received by the fuel surface from the compartment. This results in a decrease in the dependence of $\dot{m}_v$ on A_v. Since airflow rate sets an upper limit to the burning rate in the compartment, a larger fuel sample can burn in a compartment with a wider doorway before the effect of excess fuel is noted.

The corresponding theory shown in figure 3b displays multivalued results indicated by dashed curves that are physically impossible. This mathematical phenomenon was displayed in this case since the solution procedure used $\dot{m}_v$ as the independent variable. Initially, as $\dot{m}_v$ was incremented, the solution yielded increasing values for A_v. But as heat transfer from the enclosure to the fuel became significant, an increase in $\dot{m}_v$ resulted in a decrease in A_v. That is, at this higher surface heat flux a smaller area was required to support this fuel supply rate. Moreover, the upper inflection point on the dashed curves marks the stoichiometric point above which excess fuel is released. One interpretation of this result is that a critical fuel area exists above which a rapid increase in the burning rate, temperature, and heat flux would occur. The state of the fire would move from a relatively small fire with sufficient air for combustion to a fire which produces excess fuel and is "ventilation controlled." Thus the steady-state model suggests one mechanism for a rapid transition in fire growth (flashover). The validity of this interpretation must be more fully explored with a transient model; however, the data in figure 3a tend to support this idea -- particularly since the "unsteady" data points are on the steepest portion of the curves.

The results for gas temperature in figure 4 demonstrate that the temperature is highest for the smallest doorway and smaller fuel areas. However, for large fuel samples, the inverse is true with regard to doorway width. Thus it is clear that the assessment of the severity of thermal conditions due to a fire is a complex function of fuel and ventilation conditions. Moreover, the agreement between theory and experiments tends to follow that of the mass loss results. This suggests that a more accurate determination of mass loss would improve temperature prediction.

Figure 5 displays the results for incident heat flux to the floor. The theoretical value was calculated as

$$\dot{q}''_F = \sigma F_{dF} \left[\epsilon_g T_g^{\,4} + (1-\epsilon_g) T_w^{\,4} - T_a^{\,4} \right] + \epsilon_f \sigma T_f^{\,4} \cdot \frac{2H_f\sqrt{\pi A_v}}{A_F} \qquad (25)$$

where the first term represents the incident flux from the upper hot layer and the second term represents the heat flux from the flame (insignificant for this scale analysis). The disparity in agreement here is due to the inaccuracy of the temperature prediction.

Figure 6 shows good agreement between theory and the data for airflow. However, that is based on empirical selection of the entrainment relationship (eq. (8)). More study must be made of this aspect of the flow model.

Figure 7 is presented in a form common to results for the burning of wood cribs, i.e., as a function of compartment ventilation. For wood cribs, the data initially follow a linear plot (e.g., $\dot{m}_v \sim W_o H_o^{3/2}$) followed by horizontal lines of constant burning rate for corresponding crib sizes. The PMMA data suggest this same initial trend, but with some preferred ordering with fuel area. The compartment radiation has a pronounced effect on the PMMA burning rate at high ventilation which is markedly different from crib fires. A locus of theoretical fires with an incident floor heat flux of 2 W/cm^2 is also shown on figure 7. This corresponds approximately with the data. The utility of this plot can be appreciated if the heat flux locus is recognized as a condition for other potential ignitions within the enclosure.

Finally, the effect of radiation on the mass loss rate of PMMA is plotted in figure 8. It appears that a reduction in the oxygen concentration of the flow entrained by the fire plume reduced the mass loss rate. This is qualitatively consistent with the results obtained by Tewarson [13] with a calorimetric apparatus. In fact, despite the differences in experimental conditions, his data [14] taken under normal air conditions are in some agreement with the enclosure results, especially at high flux. The results in figure 8 can be explained by considering the mass loss rate per unit area to be directly dependent on the sum of the incident floor heat flux and the heat flux from the flame. A reduction in the oxygen would reduce the flame heat flux. This effect is not accounted for in the current model (eqs. (9) and (10)). However, the values of oxygen concentration calculated for figure 8 were based on the rate of mixing between the hot upper layer and the jet of induced airflow at the doorway. The mixing rate was determined from measurements taken in a similar experimental configuration (appendix B) [15].

In conclusion, the theory presented yields good qualitative results when compared with the data. Weak features of the model appear consistent with the accuracy of the results. Improvements in the models for radiative transport, particularly from the flame, should improve the results. Also in the flow model, plume entrainment needs to be better understood along with mixing within the compartment. Finally, the effect of oxygen depletion on burning should be included. In general, it appears that a conceptual basis for predicting features of fires in compartments has been established and with refinement should lead to more accurate results.

6. REFERENCES

[1] Quintiere, J. G., Growth of fire in building compartments. Fire Standards and Safety, ASTM STP 614, 131-167 (1977).

[2] Gross, D. and Robertson, A. F., Tenth Symposium (International) on Combustion, 931-942, The Combustion Institute (1965).

[3] Thomas, P. H. and Nilsson, L., Fully developed compartment fires: new correlations of burning rates, F.R. Note No. 979, Fire Research Station, Borehamwood, England (Aug. 1973).

[4] Friedman, R., Behavior of fires in compartments, International Symposium Fire Safety of Combustible Materials, 100-113, Edinburgh, Scotland (Oct. 15-17, 1975).

[5] Tewarson, A., Combustion and Flame, Vol. 19, 363-371 (1972).

[6] Takeda, H. and Nakaya, I., Small-scale model fire in enclosure using liquid fuel - effect of ventilation factor, Paper presented at the Second Joint Meeting of the U.S. - Japan Panel on Fire Research and Safety, UJNR, Tokyo (Oct. 19-22, 1976).

[7] Tanaka, T., A mathematical model of a compartment fire, BRI Research Paper No. 70, Ministry of Construction, Japanese Government (Feb. 1977).

[8] Emmons, H. W., Mitler, H. E., and Trefethen, L. N., Computer fire code III, Home Fire Project Technical Report No. 25, Harvard University, Cambridge, Mass. (Jan. 1978).

[9] McCaffrey, B. J. and Rockett, J. A., J. Research, National Bureau Standards (U.S.), Vol. 82, No. 2, 107-117 (1977).

[10] Prahl, J. and Emmons, H. W., Combustion and Flame, Vol. 25, No. 3, 369-385 (Dec. 1975).

[11] Rockett, J. A., Combustion Science and Technology, Vol. 12, 165 (1976).

[12] Steward, F. R., Combustion Science and Technology, Vol. 2, 203 (1970).

[13] Tewarson, A. and Pion, R. F., Combustion and Flame, Vol. 26, 85-103 (1976).

[14] Tewarson, A., Fire and Materials, Vol. 1, 90 (1976).

[15] McCaffrey, B. J. and Quintiere, J. G., Heat Transfer and Turbulent Buoyant Convection, Vol. II, 457-472, Hemisphere (1977).

[16] Modak, A. T. and Croce, P. A.: Plastic Pool Fires. FMRC Serial No. 22361-3, Factory Mutual Research, Norwood, Mass., June 1976.

[17] Markstein, G. H., Radiative properties of plastic fires, Seventeenth Symposium (International) on Combustion, The Combustion Institute (to be presented).

[18] Zukoski, E. E. and Kubota, T., An experimental investigation of the heat transfer from a buoyant gas plume to a horizontal ceiling - part 2. Effects of ceiling layer, Progress Report. Grant No. 5-9004, National Bureau of Standards (U.S.) (June - Sept. 1975).

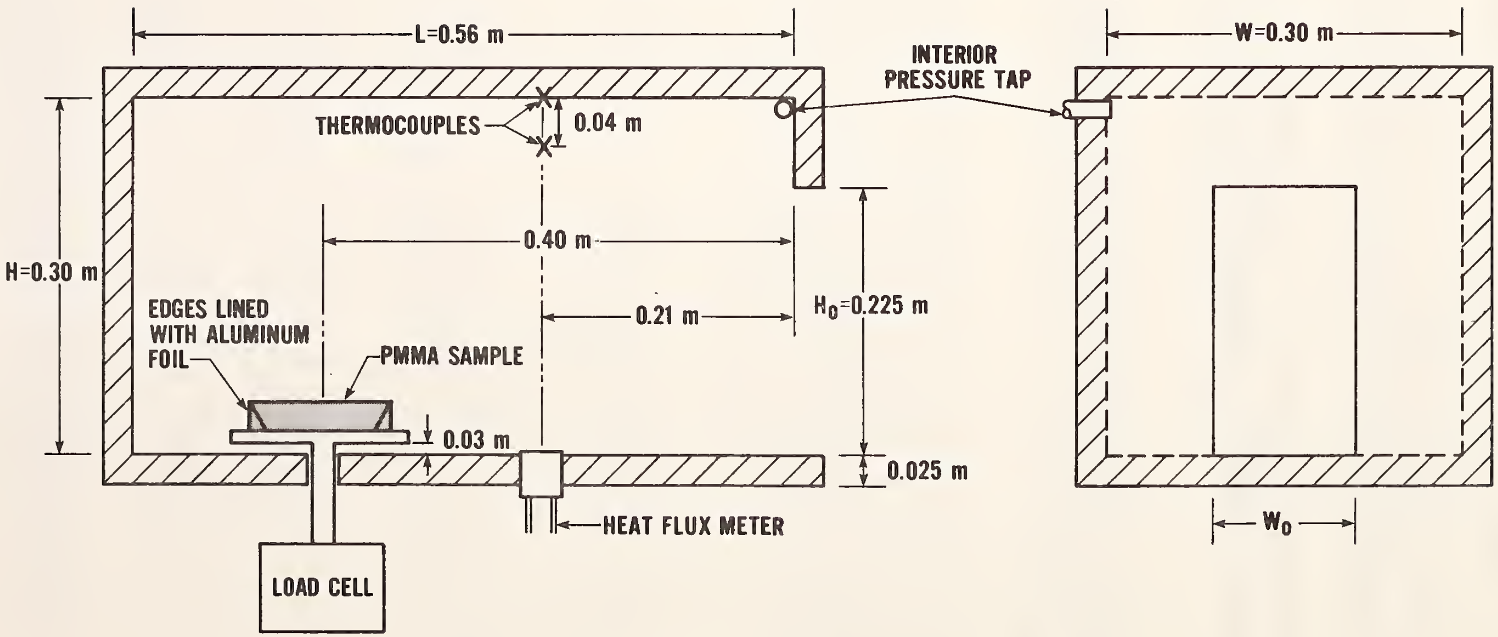

Figure 1. Experimental arrangement

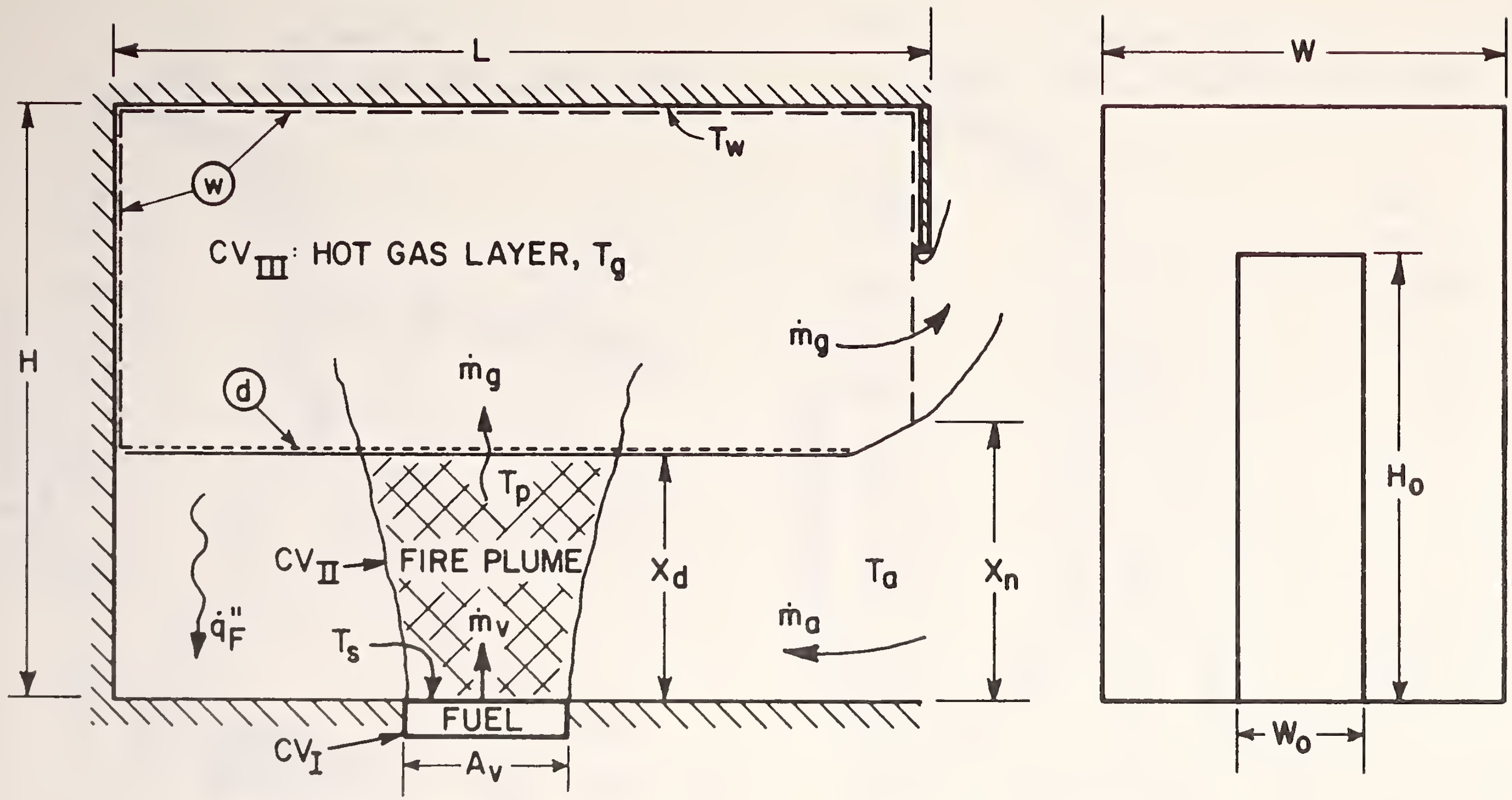

Figure 2. Control volumes (CV) used in the mathematical model

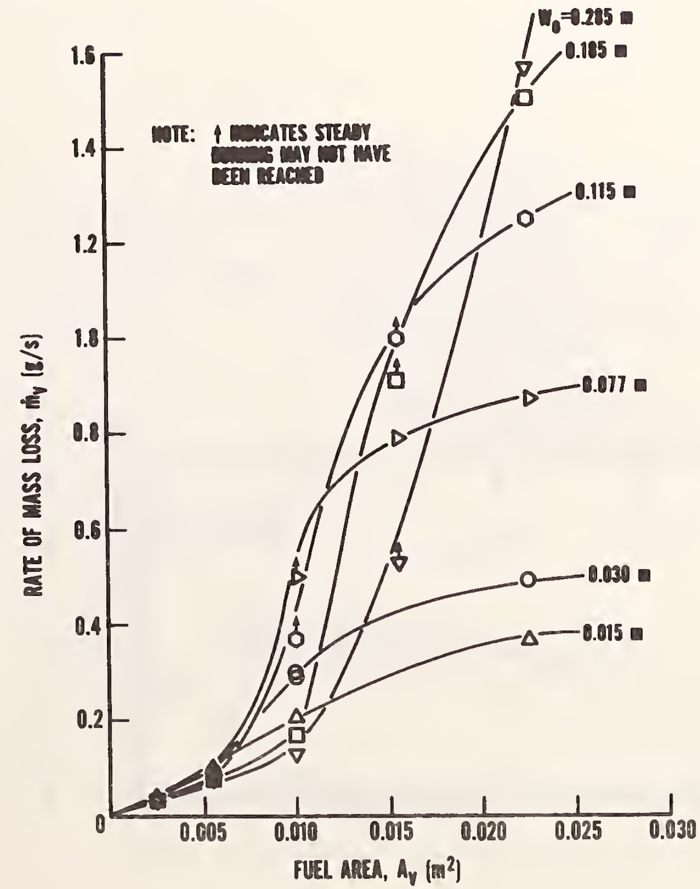

Figure 3a. Experimental results for rate of mass loss

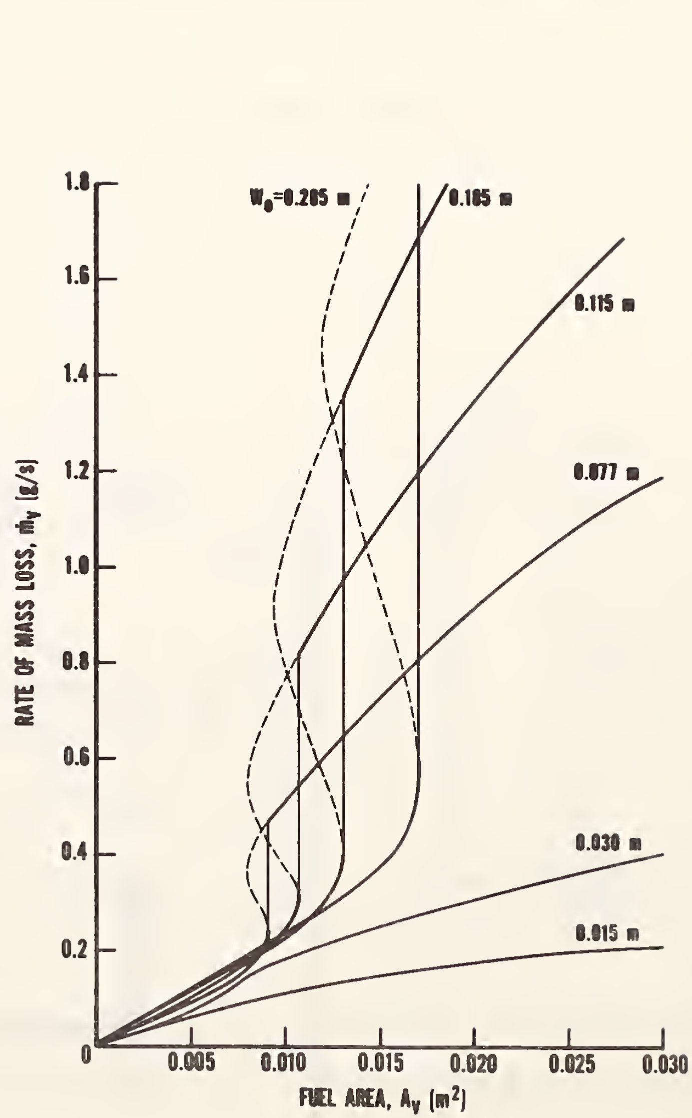

Figure 3b. Theoretical results for rate of mass loss

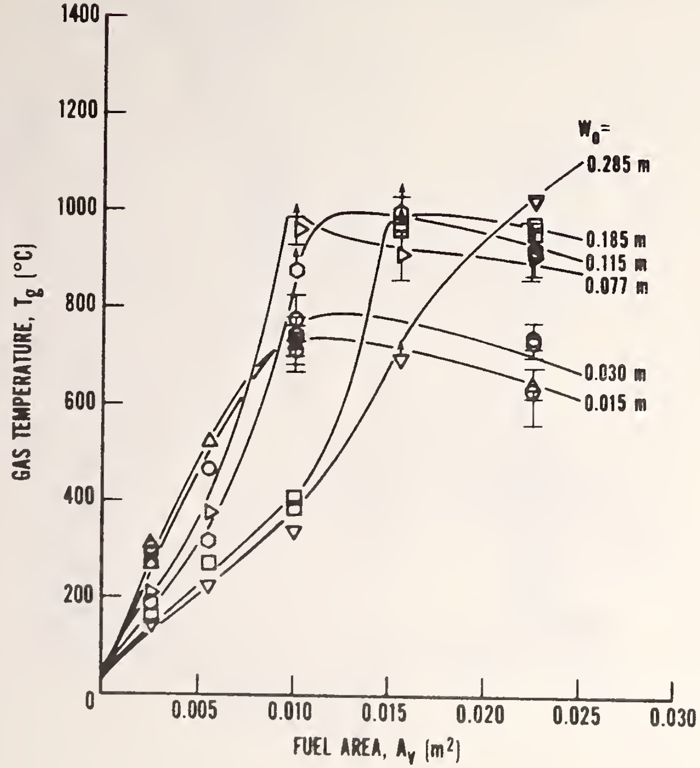

Figure 4a. Experimental results for gas temperature

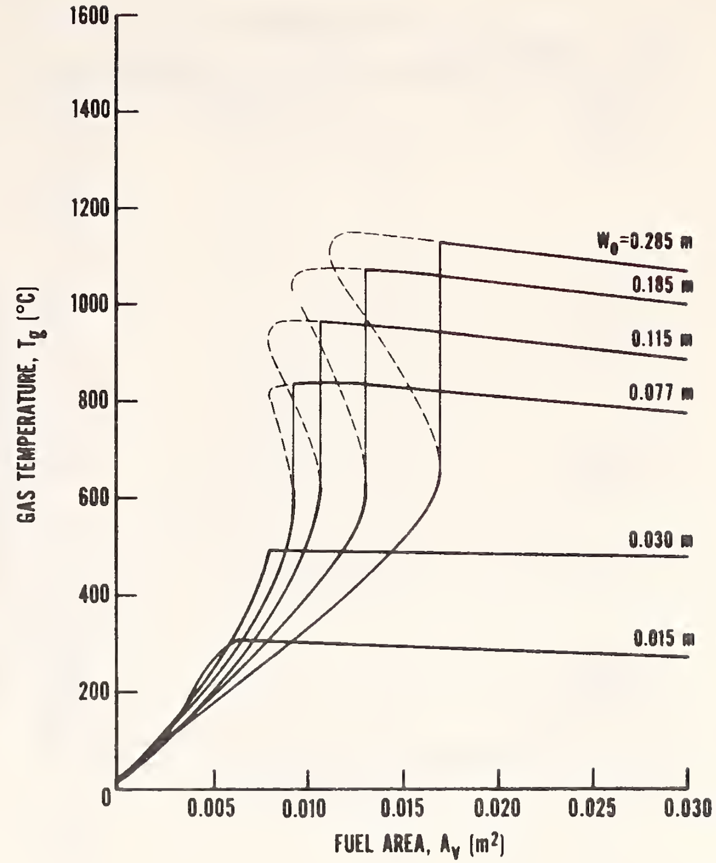

Figure 4b. Theoretical results for gas temperature

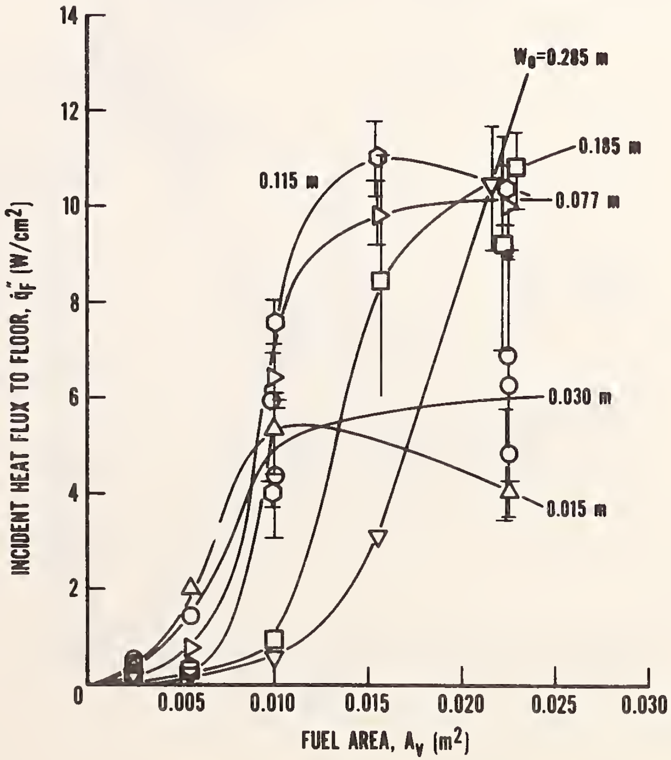

Figure 5a. Experimental results for incident heat flux to the floor

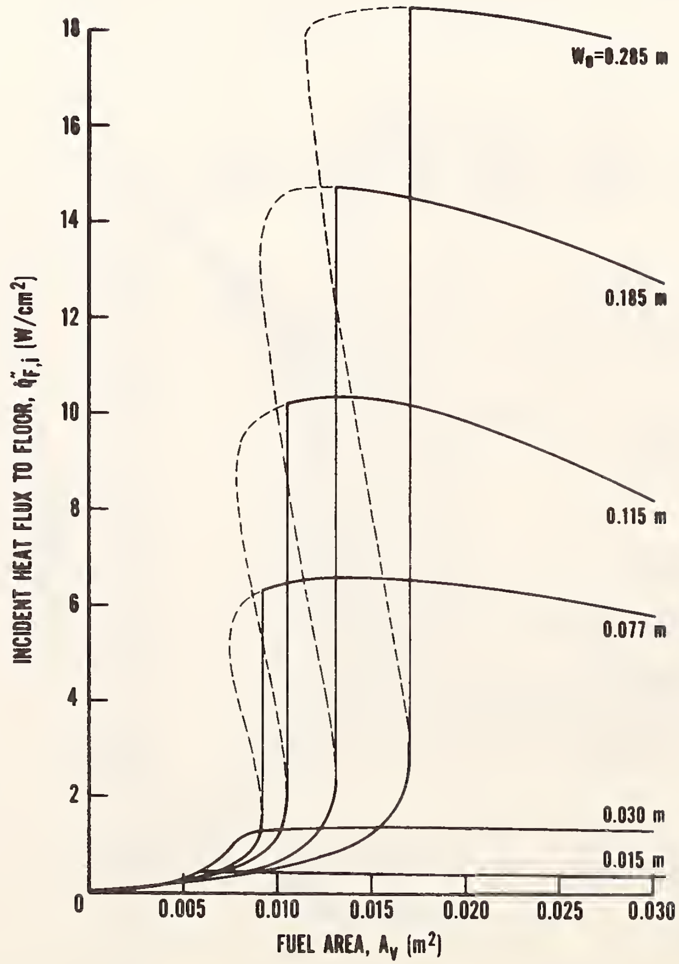

Figure 5b. Theoretical results for incident heat flux to the floor

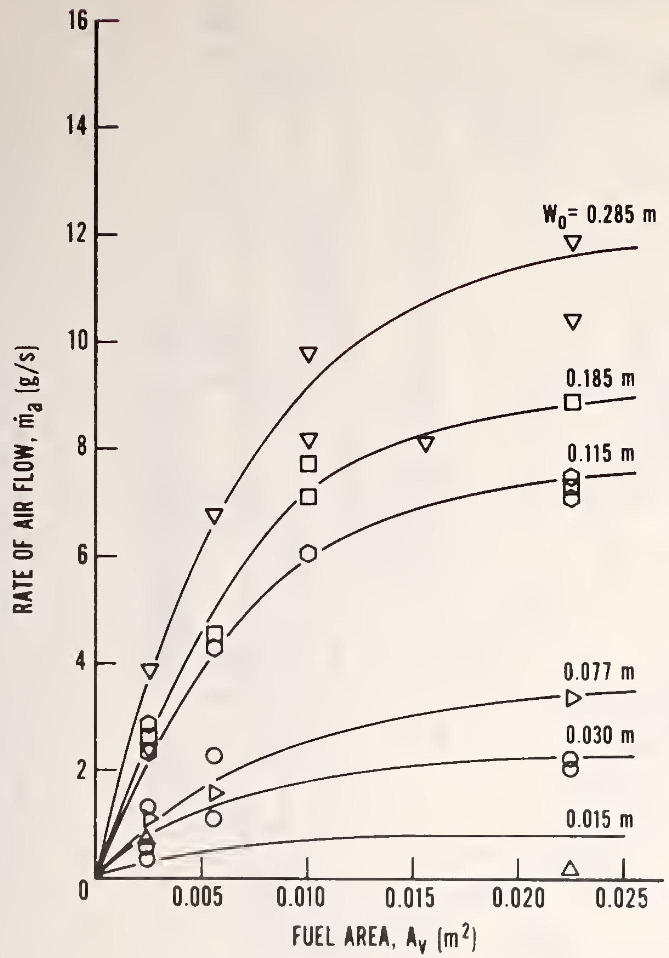

Figure 6a. Experimental results for rate of induced airflow

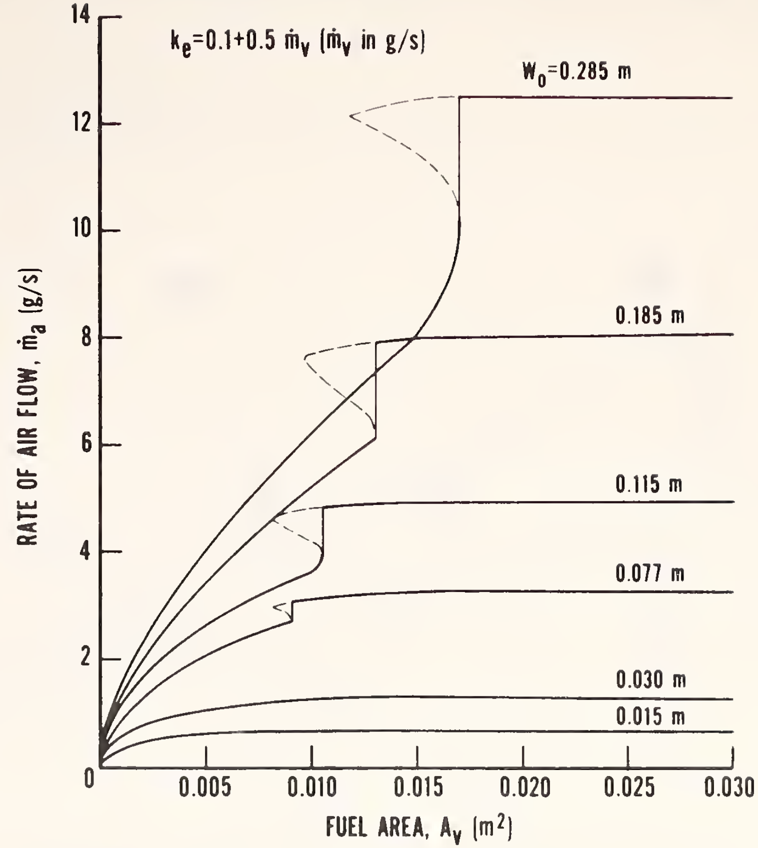

Figure 6b. Theoretical results for rate of induced airflow

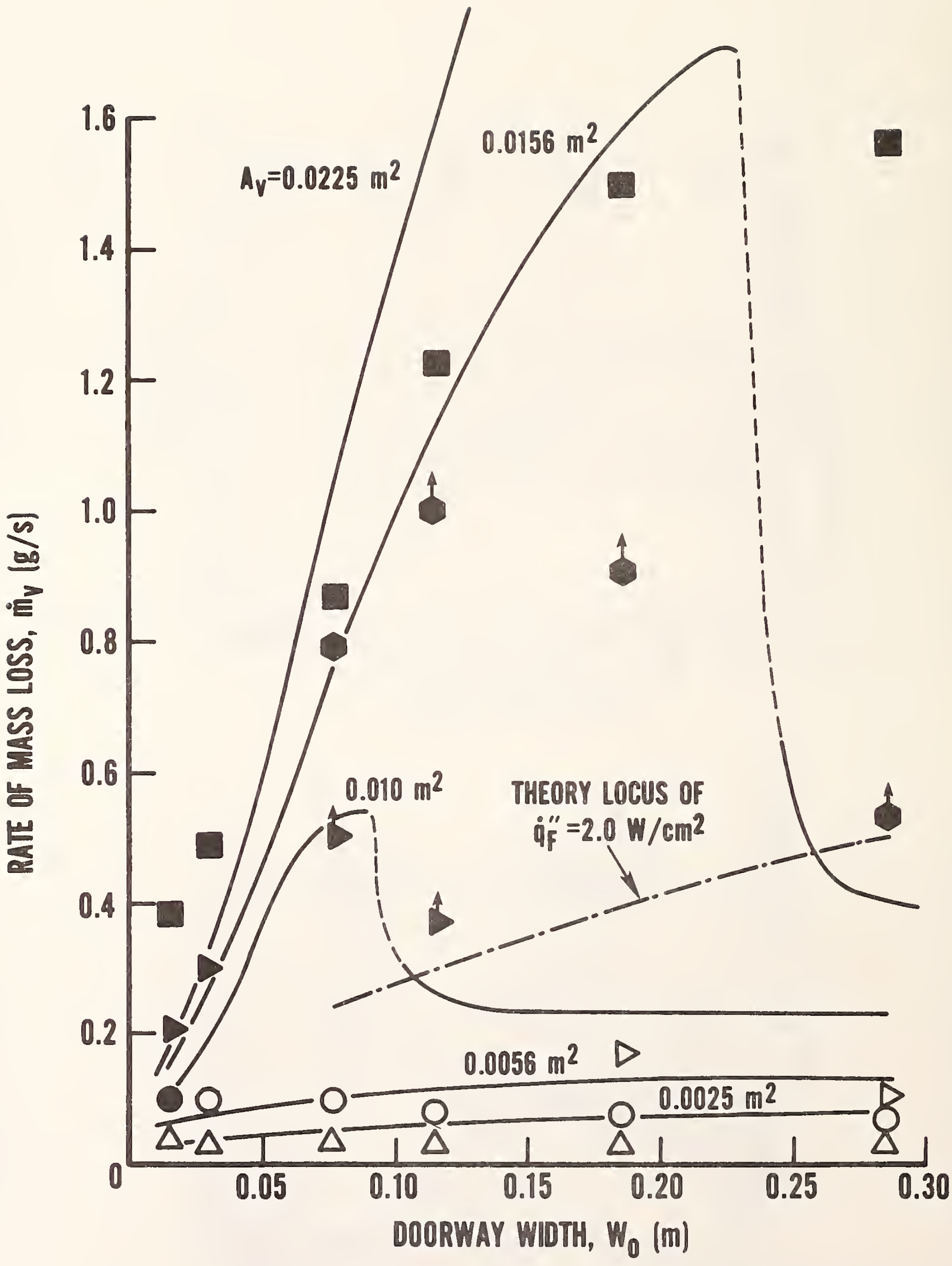

Figure 7. Fuel mass loss rate as a function of ventilation and fuel area. Theory: —— Data: △ - 0.0025 m², ○ - 0.0056 m², ▷ - 0.0100 m², ⬡ - 0.0156 m², □ - 0.0225 m². Open symbols represent data less than 2.0 W/cm². Shaded symbols represent data greater than 2.0 W/cm².

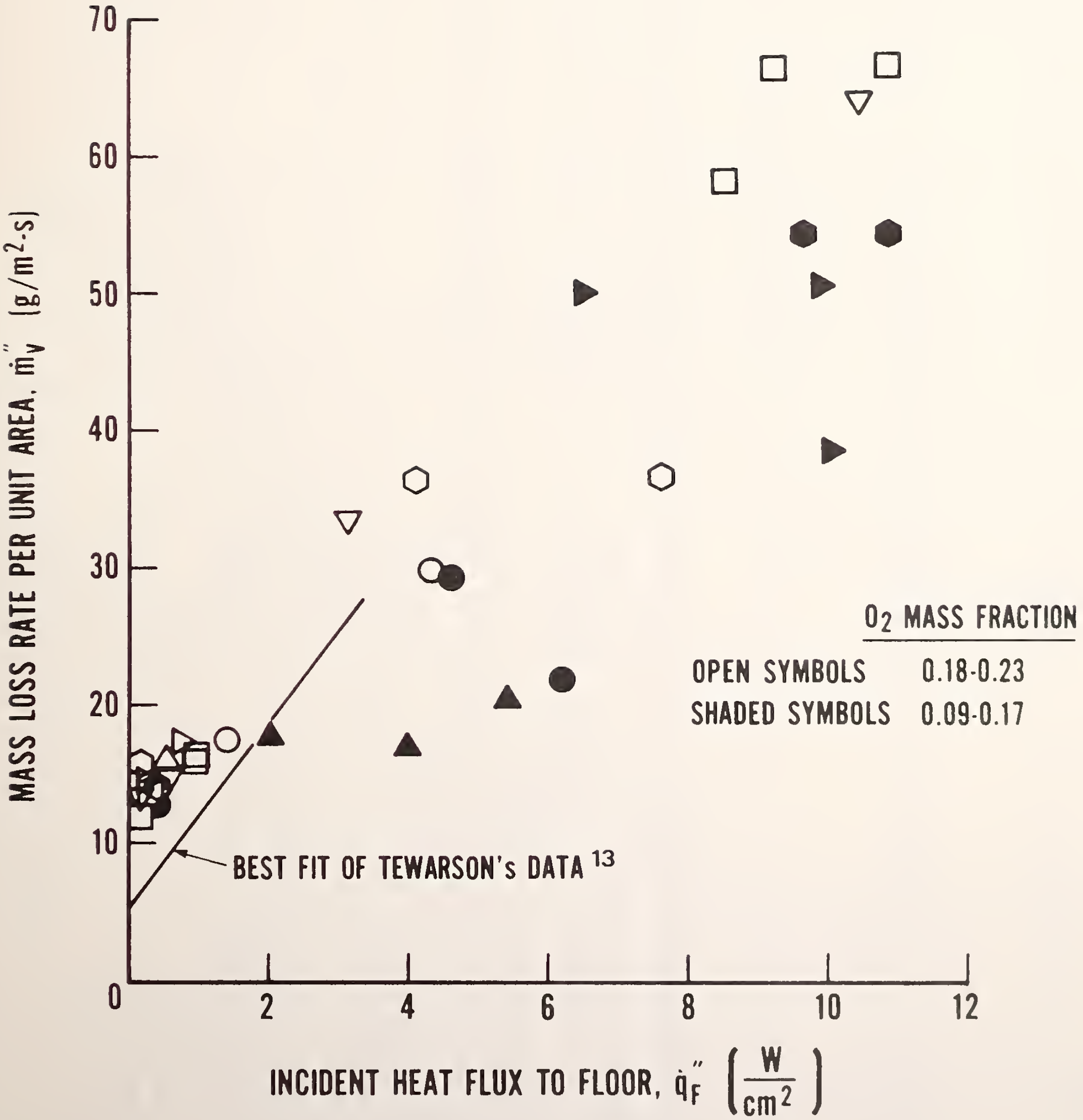

Figure 8. Fuel mass loss per unit as a function of incident heat flux. (The oxygen concentration in the flow entrained by the fire plume was estimated.)

TABLE I

Summary of experimental results

Exp No.	W_o Doorway Width	A_v Fuel Area	Duration of Burn	Duration of Steady Burning	$\dot{m}_v$ Steady Mass Loss Rate	T_g Gas Temperature	T_w Ceiling Temperature	$\dot{q}''_F$ Incident Floor Heat Flux	Δp Maximum Room Pressure Rise	$\dot{m}_a$ Calculated Air Flow Rate
	m	m²	min	min	g/s	°C	°C	W/cm²	N/m²	g/s
15	0.015	0.0025	26	-	(0.040)	270 ± 5	202 ± 10	0.39 ± .07	1.16 ± .04	0.712
14		0.0025	26	-	(0.040)	280 ± 10	212 ± 10	0.39 ± .07	1.16 ± .08	0.680
5A		0.0025	26	6.5	0.040	315 ± 12	245 ± 12	0.54 ± .07	[0.68 ± .08]	-
6A		0.0056	25	5	0.100	522 ± 12	450 ± 12	2.01 ± .12/.35	-	-
4A		0.0100	22	4	0.207	725 ± 25	660 ± 25	5.40 ± .69/1.15	-	-
7A		0.0225	23	6	0.383	645 ± 35	590 ± 50	4.03 ± .58	1.48 ± .32	0.157
1	0.030	0.0025	>20*	-	(0.032)	300 ± 10	235 ± 20	0.52 ± .03/.04	1.16 ± .04	1.30
2		0.0025	>19*	-	(0.032)	275 ± 10	205 ± 5	0.40 ± .01	1.12 ± .04	1.34
1A		0.0025	27	9	0.032	285 ± 5	212 ± 10	0.40 ± .02/.07	0.84 ± .08	0.54
8A		0.0056	24	4	0.098	463 ± 5	393 ± 12	1.43 ± .07/.12	1.31 ± .04	1.01
2A		0.0100	20	3	0.300	717 ± 50	645 ± 60	4.37 ± 1.4	-	-
6		0.0100	19.5	-	(0.30)	778 ± 50	730 ± 50	5.98 ± .23	2.16 ± .08	2.01
9A		0.0100	18	3	0.292	732 ± 50	683 ± 50	4.60 ± 1.2	[1.44 ± 0]	-
3A		0.0225	19	2	(0.490)	730 ± 35	680 ± 50	4.83 ± .92/1.4	2.00 ± 0	1.54
10A		0.0225	19	5	0.490	740 ± 25	700 ± 25	6.21 ± 1.2	[1.64 ± .08]	-
3		0.0225	21	-	(0.490)	635 ± 75	610 ± 75	5.75 ± 2.3	2.00 ± .08	1.78
11A	0.077	0.0025	24	6	0.037	210 ± 5	160 ± 7	0.21 ± .02/.04	0.68 ± .08	1.14
12A		0.0056	24	4	0.097	378 ± 10	288 ± 10	0.74 ± .07/.12	1.00 ± .08	1.57
13A		0.0100	16	1†	0.500	960 ± 35	778 ± 35	6.44 ± .69	[0.92 ± .12]	-
31A		0.0156	11.5	2	0.790	910 ± 50	865 ± 50	9.88 ± .65	[0.72 ± .20]	-
15A		0.0225	10	2	0.870	902 ± 25	854 ± 35	10.0 ± 9	[1.28 ± .08]	-
14A		0.0225	10	3	0.875	902 ± 50	865 ± 50	8.05 ± 1.2**	1.80 ± .12	2.53
4	0.115	0.0025	23	-	(0.038)	188 ± 5	141 ± 5	0.17 ± .01	0.72 ± .04	2.38
17A		0.0025	26	6	0.038	195 ± 5	149 ± 3	0.16 ± .01	0.76 ± .08	2.85
18A		0.0056	27	5	0.078	317 ± 7	239 ± 5	0.39 ± .03	1.12 ± 0	4.26
5		0.0100	14	-	(0.367)	876 ± 12	766 ± 25	7.59 ± .46	1.96 ± .04	6.04
16A		0.0100	17	1.5†	0.367	741 ± 10	644 ± 5	4.03 ± .30	1.68 ± .08	4.74
30A		0.0156	11	1.5†	1.000	993 ± 25	937 ± 25	11.0 ± .8	[1.00 ± .20]	-
7		0.0225	8	-	(1.225)	927 ± 50	902 ± 50	10.8 ± .23	2.24 ± .12	7.09
23A		0.0225	8	2	1.225	902 ± 50	854 ± 50	9.62 ± .78	2.24 ± .08	7.26
8	0.185	0.0025	21	-	(0.030)	158 ± 5	112 ± 5	0.23 ± .2	[0.80 ± .20]	-
19A		0.0025	28	6	0.030	154 ± 5	112 ± 3	0.09 ± .01	0.56 ± .04	2.60
20A		0.0056	27	4.5	0.075	263 ± 10	205 ± 5	0.30 ± .13	0.88 ± .08	4.42
21A		0.0100	25	5	0.163	385 ± 15	344 ± 10	0.91 ± .04/.08	1.24 ± .04	7.11
9		0.0100	22	-	(0.163)	415 ± 10	337 ± 15	0.99 ± .12	1.32 ± .12	7.75
29A		0.0156	16	1†	0.908	973 ± 25	863 ± 25	8.45 ± 1.0/2.6	[1.16 ± .08]	-
10		0.0225	6.5	-	(1.50)	975 ± 50	927 ± 50	9.2 ± 2.3	2.04 ± .04	8.87
22A		0.0225	9.5	2	1.50	950 ± 75	902 ± 50	10.8 ± .78	1.88 ± .08	7.29
11	0.285	0.0025	22	-	(0.033)	139 ± 3	100 ± 3	0.18 ± .02	0.52 ± .04	3.81
24A		0.0025	28	6	0.033	146 ± 7	110 ± 3	0.08 ± .01	0.48 ± .08	2.37
25A		0.0056	33	5	0.068	220 ± 3	170 ± 3	0.21 ± .01	0.80 ± .08	6.76
12		0.0100	25	-	(0.148)	341 ± 10	268 ± 10	0.62 ± .05/.12	1.12 ± .04	9.77
26A		0.0100	27	4	0.148	330 ± 12	268 ± 12	0.52 ± .01	1.04 ± .08	8.17
28A		0.0156	20	1†	0.527	693 ± 25	595 ± 25	3.1 ± .26	1.43 ± .08	8.18
13		0.0225	7	-	(1.56)	1034 ± 25	902 ± 25	10.4 ± .69	1.84 ± .08	10.4
27A		0.0225	8.5	2	1.56	1022 ± 25	925 ± 25/50	10.4 ± 1.3	1.92 ± .12	11.9

* Sample was extinguished before complete consumption

† May not have reached steady-state

[ ] Pressure tap clogged

( ) Estimated to calculate $\dot{m}_a$

** Water coolant hose melted

Note: Variation in the measured quantity refers to the span of values about a mean over the duration of steady burning.

TABLE II

Specified parameters for the theoretical model

		Remarks
Fuel Parameters		
r, air to fuel mass ratio	8.25	based on combustion of $C_5H_8O_2$ to CO_2 and H_2O
ΔH, heat of combustion	2.49×10^7 J/kg	based on $C_5H_8O_2$ to CO_2 and H_2O (vapor)
ΔH_v, heat of volatilization	1.008×10^6 J/kg	approximately value given by Modak and Croce[16] (1.108×10^6 J/kg)
T_s, vaporization temperature	636 K	from Modak and Croce[16]
ρ_v, density of vaporized fuel	1.92 kg/m^3	based on $C_5H_8O_2$ as a perfect gas
C_{fuel}, specific heat of solid fuel	1.46×10^3 J/kg-K	from Modak and Croce[16]
Fire Parameters		
T_f, flame temperature	1400 K	from Markstein[17]
k_f, flame absorption coefficient	1.3 m^{-1}	" "
Heat Transfer Parameters		
h_s, fuel convective heat transfer coefficient	2.5 W/m^2-K	estimate
k_g, upper layer absorption coefficient due to H_2O and CO_2	$0.30 + 4.64\, \dot{m}_b/(\dot{m}_a + 0.6\, \dot{m}_b)$	fit based on range of temperatures and CO_2, H_2O concentrations
k_{soot}, upper layer absorption coefficient due to soot	1.9 m^{-1}	estimate
K_w, wall and ceiling conductance	5 W/m^2-K	estimate
h_F, floor convective heat transfer coefficient	10 W/m^2-K	estimate
h_w, wall and ceiling convective heat transfer coefficient	$14.4\, (\dot{m}_b \Delta H, kW)^{1/3}$ W/m^2-K	from Zukoski and Kubota[18]
Flow Parameters		
c, doorway flow coefficient	0.7	from Prahl and Emmons[10]
k_e, plume entrainment constant	$0.1 + 0.5\, (\dot{m}_v$, g/s)	empirical fit from McCaffrey and Rockett[9]
Fluid Parameters		
C_g, air and combustion product specific heat	1.046×10^3 J/kg-K	--
ρ_a, density of air	1.25 kg/m^3	--
T_a, temperature of air	300 K	--
Compartment Parameters		
H, height	0.30 m	
W, width	0.30 m	
L, length	0.56 m	
H_o, doorway height	0.225 m	
W_o, doorway width	0.015 - 0.285 m	
k_w, thermal conductivity	0.14 W/m -K	
ρ_w, density	260 kg/m^3	
δ, thickness	0.025 m	

APPENDIX A - TYPICAL EXPERIMENTAL RESULTS

Three experimental conditions have been selected to illustrate the general characteristics of the data recorded over the duration of an experimental run. For illustration, the doorway condition $W_o = 0.077$ m was selected for three fuel areas: 0.0056, 0.010, and 0.0225 m^2. The smallest area exhibited the first mode of burning, while the largest area sample exhibited the second mode of burning. The intermediate sample size appeared transitional, and did not necessarily reach a steady state.

The results are shown in figures A-1, A-2, and A-3. These plots have been traced from the continuous data records and converted into the units of the physical variable measured. It could be anticipated that the radiant heat flux would be very sensitive to temperature since $\dot{q}'' \sim T_g^4$ and that the room pressure difference would be relatively insensitive to temperature since $\Delta p \sim 1 - T_a/T_g$ by eq. (1). These trends are confirmed by the results. Also the good reproducibility of the results is indicated in figure A-3.

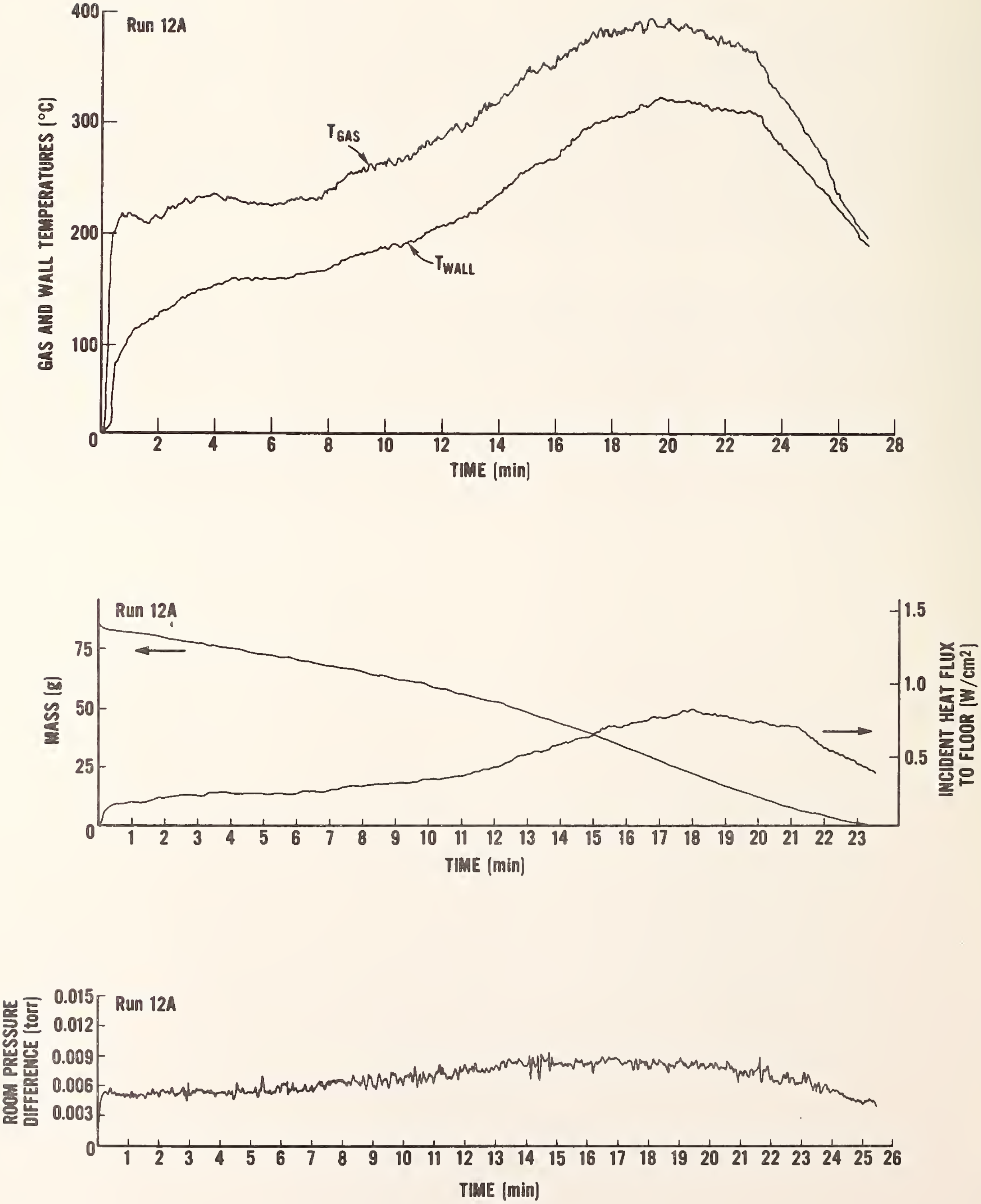

Figure A-1. Experimental results for W_o = 0.077 m and A_v = 0.0056 m^2

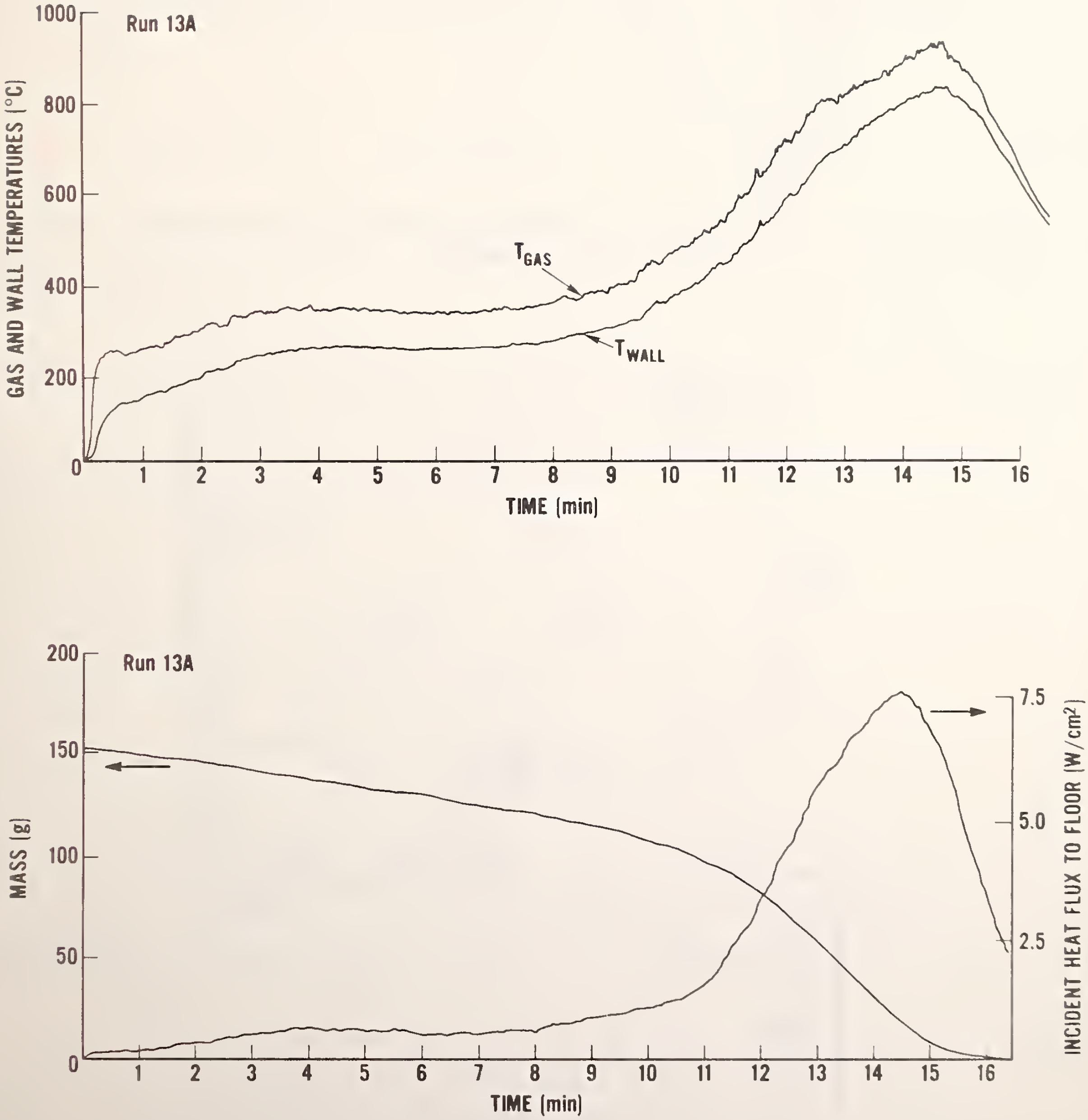

Figure A-2. Experimental results for W_o = 0.077 m and A_v = 0.010 m

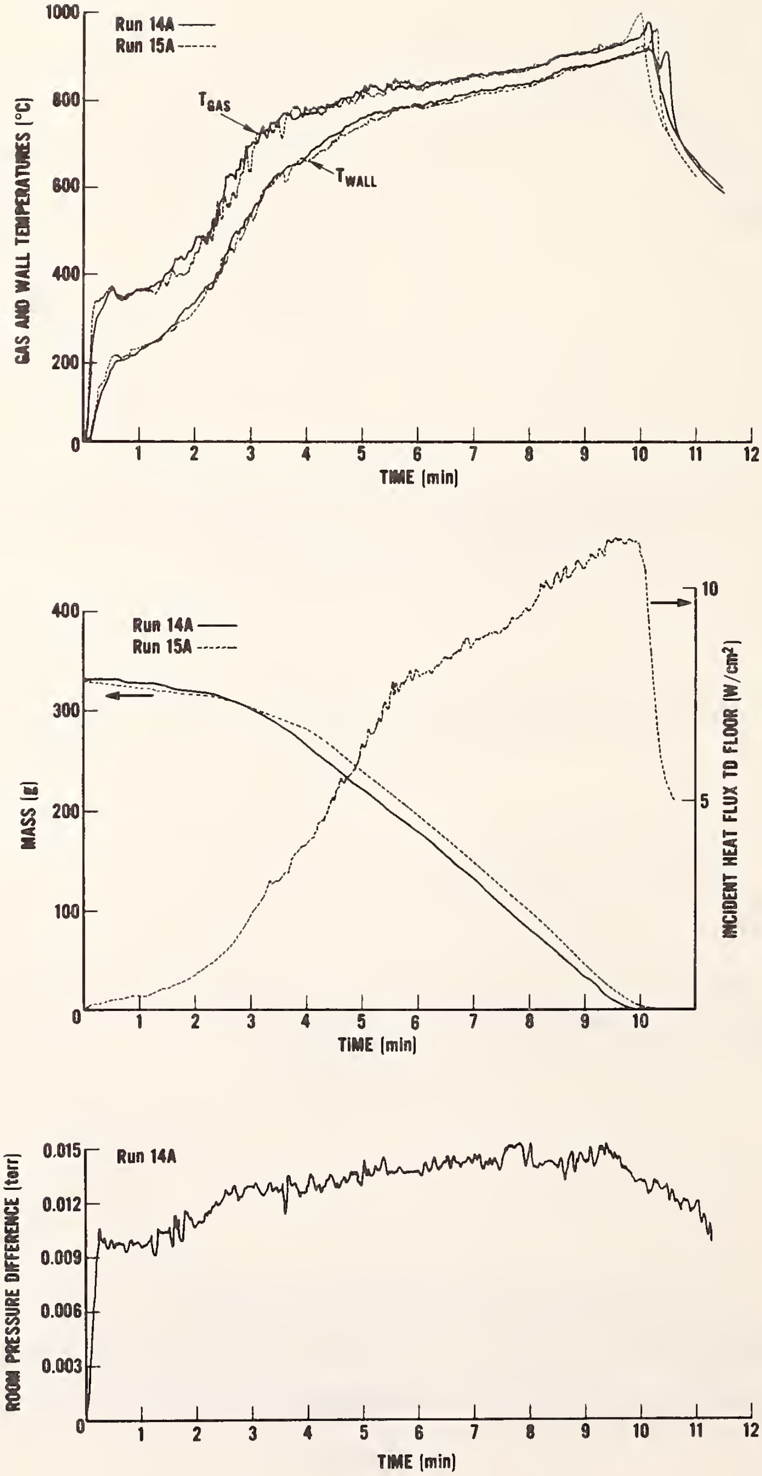

Figure A-3. Experimental results for W_o = 0.077 m and A_v = 0.0225 m^2

APPENDIX B. ESTIMATE OF THE OXYGEN CONCENTRATION OF THE FIRE PLUME ENTRAINED FLOW

As air enters the doorway of the enclosure it mixes with some hot fluid resulting in a vitiated air layer along the floor. This flow is then entrained into the fire plume. This vitiated air would reduce the energy release and thus affect the fuel mass loss rate. A simple model for this (based on eq. (9)) suggests that the rate of mass loss per unit area ($\dot{m}_v''$) is proportional to the heat flux from the flame ($\dot{q}_f''$) and the enclosure ($\dot{q}''_{enclosure}$),

$$\dot{m}_v'' \sim \dot{q}_f'' + \dot{q}''_{enclosure}. \qquad \text{(B-1)}$$

For a fixed heat flux from the surroundings, a reduction in the oxygen concentration would reduce $\dot{q}_f''$. This is consistent with the results of Tewarson and Pion [13].

It is believed that the data shown in figure 8 follow the model given by eq. (B-1). To establish this relationship, the oxygen concentration of the entrained vitiated air must be determined. The following analysis attempts to estimate this concentration.

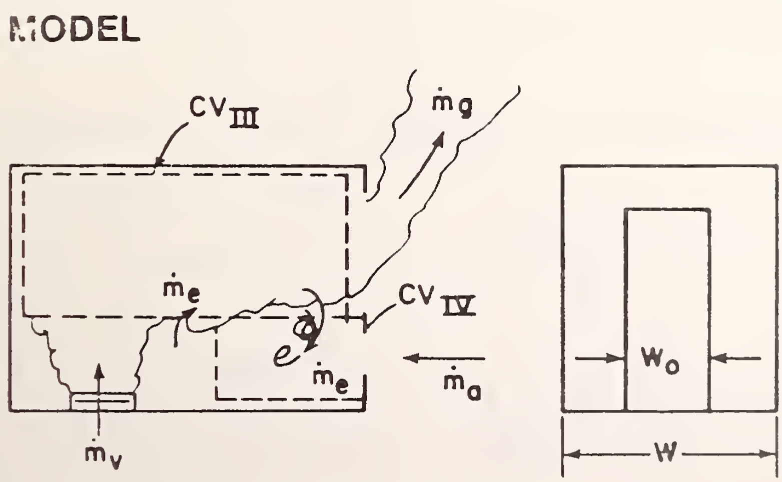

Assumptions: (1) Upper layer is well stirred at a uniform O_2 concentration.

(2) Air enters at the doorway and is contaminated by gases entrained from the upper layer.

(3) The entrained fluid is well mixed with the incoming air but only a mass flow rate equal to $\dot{m}_a$ is entrained into the fire plume and mass flow rate $\dot{m}_e$ is recirculated.

Oxygen specie conservation for CV_{IV}

[Oxygen In] = [Oxygen Out]

$$0.23\ \dot{m}_a + \phi_g\ \dot{m}_e = \phi_a\ (\dot{m}_a + \dot{m}_e) \tag{B-2}$$

where

ϕ_g is the oxygen mass concentration in the upper layer (CV_{III}).

and

ϕ_a is the oxygen mass concentration leaving CV_{IV} and entrained into the fire plume.

Oxygen specie concentration for CV_{III}

$$\begin{bmatrix} O_2 \text{ supplied} \\ \text{to fire } (CV_{II}) \end{bmatrix} - \begin{bmatrix} O_2 \text{ consumed} \\ \text{in fire } (CV_{II}) \end{bmatrix} + \begin{bmatrix} O_2 \text{ recirculated} \end{bmatrix} = \begin{bmatrix} O_2 \text{ out} \end{bmatrix}$$

$$\phi_a\ \dot{m}_a - 0.23\ r\dot{m}_v + (\phi_a - \phi_g)\ \dot{m}_e = \phi_g\ \dot{m}_g \tag{B-3}$$

Solving these equations results in:

For excess air, $\dot{m}_v \leq \dfrac{\phi_a \dot{m}_a}{0.23r}$

$$\phi_g = \frac{0.23\ (\dot{m}_a - r\dot{m}_v)}{\dot{m}_a + \dot{m}_v} \tag{B-4}$$

and

$$\phi_a = 0.23 \left[\left(\frac{\dot{m}_a}{\dot{m}_a + \dot{m}_e} \right) + \frac{(\dot{m}_a - r\dot{m}_v)\ \dot{m}_e}{(\dot{m}_a + \dot{m}_v)\ (\dot{m}_a + \dot{m}_e)} \right] \tag{B-5}$$

For insufficient air, $\dot{m}_v > \dfrac{\phi_a\ \dot{m}_a}{0.23r}$

$$\phi_g = 0 \tag{B-6}$$

and

$$\phi_a = 0.23 \left(\frac{\dot{m}_a}{m_a + m_e} \right) . \tag{B-7}$$

Finally, the entrained flow was estimated from the measurements made in a similar scale experiment and doorway configuration [15]. These results are presented in table B-1 as fractions of the doorway airflow rate. The fractional factor is given as a function of the width ratio W_o/W.

$$\dot{m}_e = f \cdot \dot{m}_a \qquad \text{(B-8)}$$

Table B-1. Estimated entrainment rate

W_o (m)	W_o/W --	$f = \dot{m}_e/\dot{m}_a$ --
0.015	0.05	1.6
0.030	0.10	1.2
0.077	0.257	0.5
0.115	0.383	0.4
0.185	0.617	0.3
0.285	0.95	0.2

The values of ϕ_a and ϕ_g were then determined from the experimental airflow rate and equations given above. The results of those calculations are given in table B-2. From those results as shown plotted in figure B-1, it is clear that for large fires and small doorway widths, the entrained flow into fire has a low oxygen concentration. The effect of this vitiated air on fuel mass loss was shown in figure 8 by discriminating between a high and low set of oxygen concentration values in the data. A closer examination of the results may indicate a more continuous effect of reduced oxygen on mass loss but there are some exceptions in the data. In general, the effect of oxygen appears to have been demonstrated.

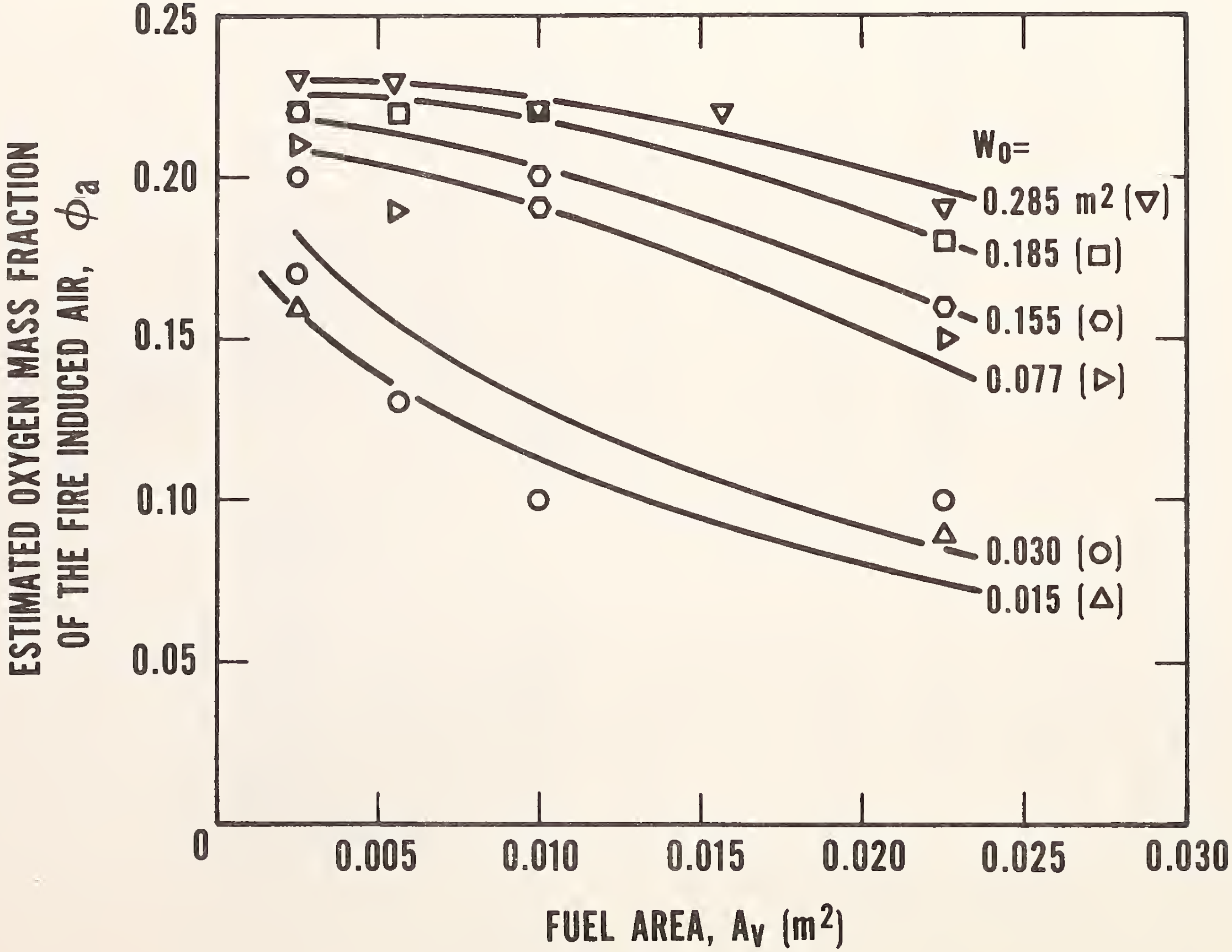

Figure B-1. Estimated oxygen concentration for the flow induced into the flame

Table B-2. Calculated oxygen mass concentrations

Exp. No.	W_o Doorway Width (m)	A_v Fuel Area (m^2)	[illegible]$_g$ Calculated O_2 Mass Conc. --	[illegible]$_a$ Calculated O_2 Mass Conc. --
15	0.015	0.0025	0.12	0.16
14		0.0025	0.11	0.16
5A		0.0025	--	--
6A		0.0056	--	--
4A		0.0100	--	--
7A		0.0225	0.0	0.09
1	0.030	0.0025	0.18	0.20
2		0.0025	0.18	0.20
1A		0.0025	0.11	0.17
8A		0.0056	0.04	0.13
2A		0.0100	--	--
6		0.0100	0.0	0.10
9A		0.0100	--	--
3A		0.0225	0.0	0.10
10A		0.0225	--	--
3		0.0225	0.0	0.10
11A	0.077	0.0025	0.16	0.21
12A		0.0056	0.11	0.19
13A		0.0100	--	--
31A		0.0156	--	--
15A		0.0225	--	--
14A		0.0225	0.0	0.15
4	0.115	0.0025	0.20	0.22
17A		0.0025	0.20	0.22
18A		0.0056	--	--
5		0.0100	0.11	0.20
16A		0.0100	0.08	0.19
30A		0.0156	--	--
7		0.0225	0.0	0.16
23A		0.0225	0.0	0.16
8	0.185	0.0025	--	--
19A		0.0025	0.21	0.22
20A		0.0056	0.19	0.22
21A		0.0100	0.18	0.22
9		0.0100	0.19	0.22
29A		0.0156	--	--
10		0.0225	0.0	0.18
22A		0.0225	0.0	0.18
11	0.285	0.0025	0.21	0.23
24A		0.0025	0.20	0.23
25A		0.0056	0.21	0.23
12		0.0100	0.20	0.22
26A		0.0100	0.19	0.22
28A		0.0156	0.10	0.22
13		0.0225	0.0	0.19
27A		0.0225	0.0	0.19

APPENDIX C. CONSISTENCY OF TEMPERATURE AND HEAT FLUX DATA

Equation (25) gives an approximate expression that could be used to relate the measured gas and ceiling temperatures (T_g and T_w) with the measured floor heat flux, $\dot{q}''_F$. It can be shown that the contribution from the flame is insignificant for this small scale experiment, and the shape factor F_{dF} is between 0.7 and 1. Therefore

$$\dot{q}''_F \cong \sigma F_{dF} \left[\varepsilon_g T_g^4 + (1 - \varepsilon_g) T_w^4 \right] \qquad \text{(C-1)}$$

Also for small values of X_d ("large" fires)

$$\varepsilon_g F_{dF} \sim 0.5 (0.96) \sim 0.5$$

while for large values of X_d ("small" fires)

$$\varepsilon_g F_{dF} \sim 0.25 (0.68) \sim 0.15$$

Based on these estimates, and equating "large" and "small" fires to high and low temperature levels it follows that

$$\dot{q}''_F \sim 0.5 \ \sigma T_g^4 + 0.5 \ \sigma T_w^4 \qquad \text{(C-2)}$$

for high temperature levels;
and

$$\dot{q}''_F \sim 0.15 \ \sigma T_g^4 + 0.53 \ \sigma T_w^4 \qquad \text{(C-3)}$$

for low temperature levels.

Since T_g is greater than T_w by up to 100°C, it follows that

$$\sigma T_g^4 \geq \dot{q}''_F \geq \sigma T_w^4$$

is true for high temperature, and almost true at the lower temperature levels in these experiments. Figures C-1 and C-2 seem to follow that trend. Moreover, since T_w and T_g are of similar magnitude, $\dot{q}''_F$ plotted against either T_w or T_g tends to follow a fourth power relationship.

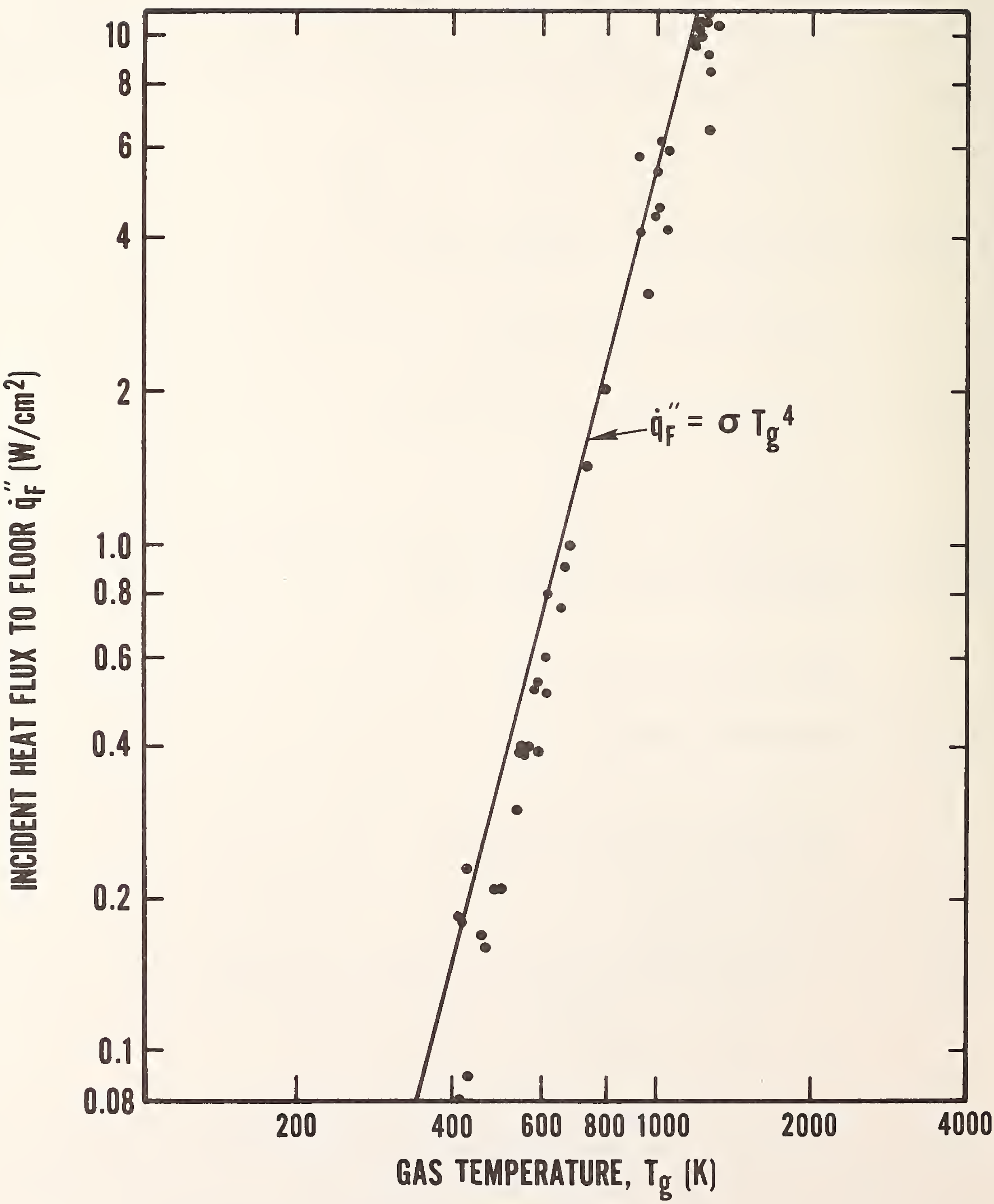

Figure C-1. Measured incident heat flux to a water cooled sensor as a function of the upper gas temperature

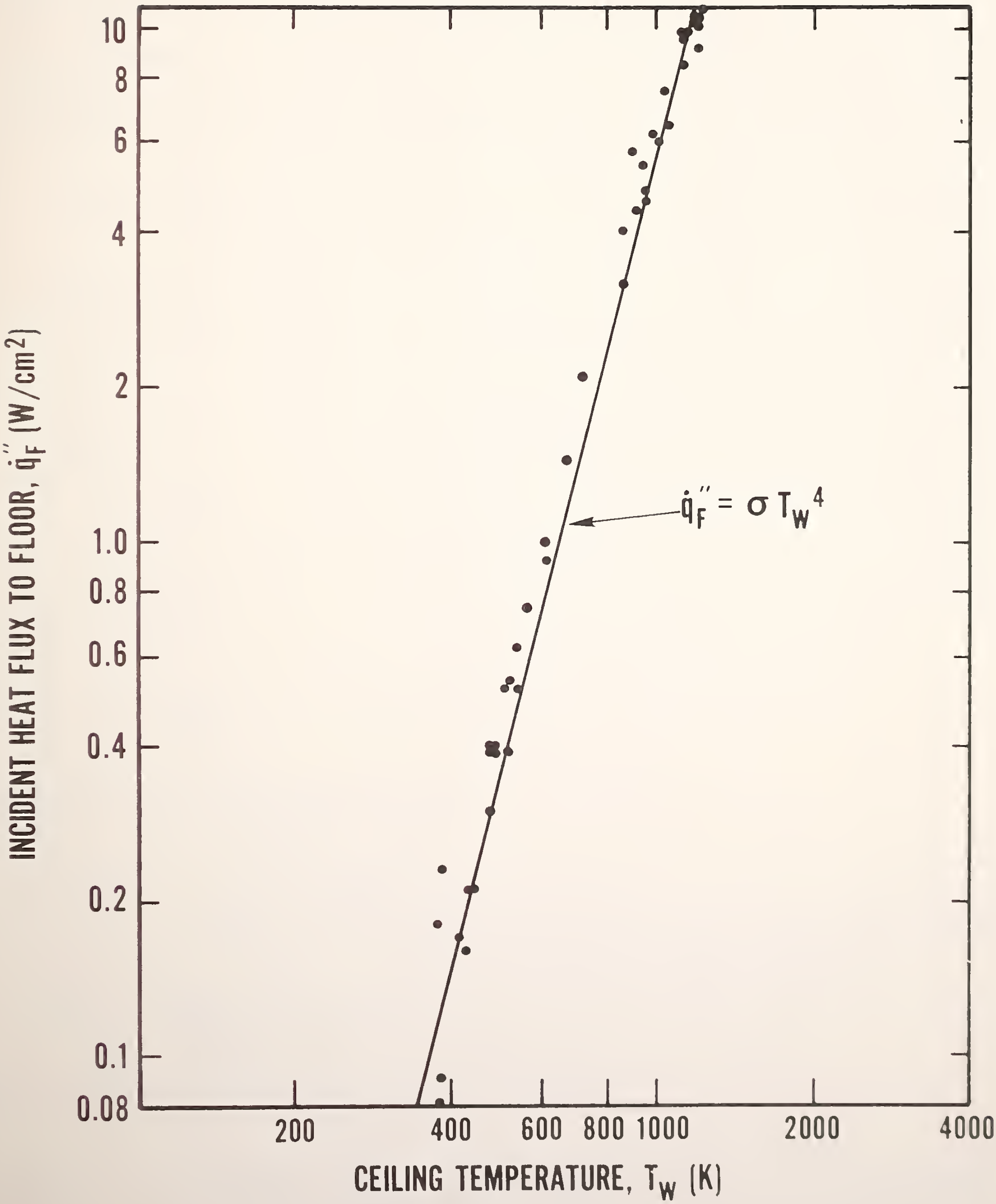

Figure C-2. Measured incident heat flux to a water cooled sensor as a function of the upper ceiling temperature

APPENDIX D. SOLUTION OF THE EQUATIONS

This section outlines the method of solution.

Flow Equations: eqs. (2) - (7)

Introduce dimensionless variables as

$$M_a = \frac{\dot{m}_a}{\dot{m}_{max}} \tag{D-1}$$

$$M_v = \frac{\dot{m}_v}{\dot{m}_{max}} \tag{D-2}$$

where

$$\dot{m}_{max} = \frac{2}{3} \; c \; \sqrt{2g} \; \rho_a \; W_o \; H_o^{3/2} \tag{D-3}$$

Also

$$y = \frac{X_n}{H_o} \tag{D-4}$$

$$z = \frac{X_d}{H_o} \tag{D-5}$$

and

$$d = \frac{T_a}{T_g} \tag{D-6}$$

The resulting three equations follow:

$$M_a + M_v = \sqrt{d(1-d)} \; (1-y)^{3/2} \tag{D-7}$$

$$M_a = \sqrt{1-d} \; (y-z)^{1/2} \left(y+\frac{z}{2}\right) \tag{D-8}$$

$$M_a = \left(\frac{\rho_a}{\rho_v}\right) \omega M_v \; (\beta z+1)^{5/2} \tag{D-9}$$

Squaring eqs. (8) and (9) and combining yields

$$f(y,z) = (y-z)\left(y+\frac{z}{2}\right)^2 - \left[\left(\frac{\rho_a}{\rho_v}\right) \omega M_v\right]^2 \frac{(\beta z+1)^5}{(1-d)} = 0 \tag{D-10}$$

And combining eqs. (7) and (9) gives

$$y = 1 - \frac{M_v^{2/3}}{d(1-d)^{1/3}} \left[1 + \left(\frac{\rho_a}{\rho_v}\right) \omega \cdot (\beta z+1)^{5/2}\right]^{2/3} \qquad \text{(D-11)}$$

Equation (D-10) is solved by a Newton-Raphson method for z, then y is determined from eq. (D-11).

Energy Equations

The following dimensionless variables are introduced:

$$\left.\begin{array}{lll}
\Theta = \dfrac{T}{T_a} & c = \dfrac{\Delta H\ \dot{m}_{max}}{A_w \sigma T_a^{\ 4}} & j = \dfrac{h_s}{\sigma T_a^{\ 3}} \\[2ex]
M = \dfrac{\dot{m}}{\dot{m}_{max}} & d = \dfrac{C_g\ \dot{m}_{max}}{A_w \sigma T_a^{\ 3}} & s = \dfrac{H_f}{H_o} \\[2ex]
\Phi = \dot{q}''/\sigma T_a^{\ 4} & e = \dfrac{C_{fuel}\ \dot{m}_{max}}{A_w \sigma T_a^{\ 3}} & p = \dfrac{A_o}{A_w} \\[2ex]
\alpha = \dfrac{A_v}{A_w} & f = \dfrac{H_o}{\sqrt{A_w}} & k = \dfrac{\sigma T_a^{\ 3} F_{dF}}{K_f} \\[2ex]
a = \dfrac{h_w}{\sigma T_a^{\ 3}} & g = \dfrac{\Delta H_v\ \dot{m}_{max}}{A_w \sigma T_a^{\ 4}} & \\[2ex]
b = \dfrac{K_w}{\sigma T_a^{\ 3}} & &
\end{array}\right\} \qquad \text{(D-12)}$$

The dimensionless equations to be solved result as follows:

From eqs. (14) and (17), along with subsidiary relationships:

$$F(\Theta_g, \Theta_w, \Theta_F) = \gamma\ \Phi_{r,d} - \varepsilon_f\ F_{dF} \left[\Phi_{r,d} + \Theta_F^{\ 4}\right] \alpha$$

$$+ b\ (\Theta_w - 1) + M_g\ d\ (\Theta_g - 1)$$

$$+ \varepsilon_f\ \Theta_f^{\ 4}\ 2\sqrt{\pi}\ s\ f\ \sqrt{\alpha} - cM_b$$

$$+ M_{py} \left[g + (e-d)\ (\Theta_s - 1)\right] + p\ \Theta_w^{\ 4} = 0 \qquad \text{(D-13)}$$

From eqs. (18) and (22):

$$G\ (\Theta_g,\Theta_w,\Theta_F) = \varepsilon_g\ \Theta_g^4 + \gamma\ (1 - \varepsilon_g)\ \Theta_F^4 - \left[1 - (1 - \gamma)\ (1 - \varepsilon_g)\right] \Theta_w^4$$

$$- \ b\ (\Theta_w - 1) + a\ (\Theta_g - \Theta_w) = 0 \tag{D-14}$$

From eq. (24):

$$H\ (\Theta_g,\Theta_w,\Theta_F) = \Theta_F - 1 - k\ \Phi_{r,d} = 0 \tag{D-15}$$

where from eqs. (9) and (10):

$$\alpha = \frac{M_V \left[e\ (\Theta_s - 1) + g\right]}{(1-\varepsilon_f)F_{dF} + \left[\varepsilon_g\Theta_g^4 + (1-\varepsilon_g)\Theta_w^4\right] + \varepsilon_f\ \Theta_f^4 + (1-\varepsilon_f)F_{SF}\Theta_F^4 - \Theta_s^4 + j\ (\Theta_f-\Theta_s)} \tag{D-16}$$

and from eq. (20):

$$\Phi_{r,d} = \varepsilon_g\ \Theta_g^4 + (1 - \varepsilon_g)\ \Theta_w^4 - \Theta_F^4\ . \tag{D-17}$$

Equations (D-13) (D-14) and (D-15) are solved by a Newton-Raphson method for Θ_g, Θ_w, and Θ_F. α is then determined from these results.

APPENDIX E. COMPUTER CODE

Please note the following about the computer code:

1) A small change was made in eq. (D-13). The term $p\Theta_w^4$ was replaced by $p(\varepsilon_g \Theta_g^4 + (1 - \varepsilon_g) \Theta_w^4)$. Hence, results are not precisely those calculated for the graphs. Resulting changes were minor.

2) For the smallest doorway, temperature and flow equation solutions for the highest mass flows did not converge (numbers 17-20 on output).

FLOW CHART

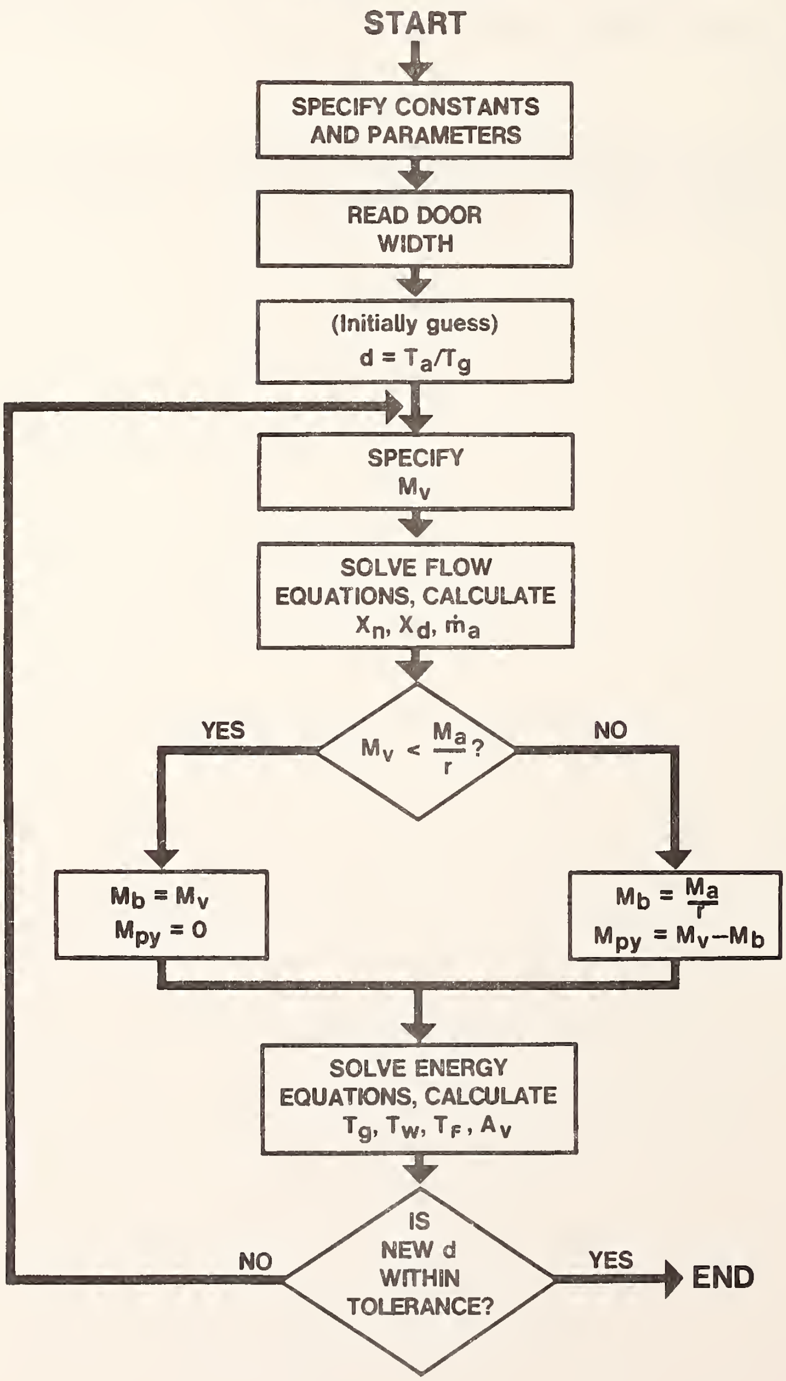
START
SPECIFY CONSTANTS AND PARAMETERS
READ DOOR WIDTH
(Initially guess) d = Ta/Tg
SPECIFY Mv
SOLVE FLOW EQUATIONS, CALCULATE Xn, Xd, ṁa
Mv < Ma/r ?
YES
NO
Mb = Mv
Mpy = 0
Mb = Ma/r
Mpy = Mv–Mb
SOLVE ENERGY EQUATIONS, CALCULATE Tg, Tw, TF, Av
IS NEW d WITHIN TOLERANCE?
NO
YES
END

Nomenclature for Program

Main Program:

Program	Theory
A	a
AF	A_F
ALPHA	α
AMASS	$\dot{m}_a$
AV	A_v
AW	A_w
B	b
BETA	β
BMASS	$\dot{m}_b$
C	c
CFUEL	c_{fuel}
CG	c_g
CO	c (flow coefficient)
CS	c_s
D	d
DELH	ΔH
DELHV	ΔH_v
DR	T_a/T_g
E	e
EF	ε_f
EG	ε_g
F24	F_{dF}
FF	f
FFLR	F_{SF}
FUEL	$\dot{m}_v$
GAMMA	γ
GG	g
GRAV	g
H	H
HF	H_f
HFLR	h_f
HO	H_o
HS	h_s
HW	h_w

Program	Theory
KE	k_e
KFLR	K_F
KG	k_g
KW	K_w
L	L
MA	M_a
MAX	$\dot{m}_{max}$
MB	M_b
MG	M_g
MPY	M_{py}
MV	M_v
OMEGA	ω
P	p
PI	π
PYMASS	$\dot{m}_{py}$
QFIRE	radiant flux from flame
QFLR	$\dot{q}''_F$ (includes flame radiation)
QR	$\dot{q}''_F$ (excludes flame radiation)
QWALL	$\dot{q}''_w$
R	r
RATIO	M_a/M_v
RD	$\Phi_{r,d}$
RF	$\Phi_{r,f}$
RFDOT	rate of radiant energy from flame
RHO	ρ_a
RHOV	ρ_v
RW	$\Phi_{r,w}$
SIGMA	σ
TA	T_a
TFLAM	T_f
TFLR	T_F
TG	T_g
THFLAM	θ_f
THFLR	θ_F
THG	θ_g
THS	θ_s
THW	θ_w
TS	T_s

Program	Theory
TW	T_w
VMASS	$\dot{m}_v$
W	W
WO	W_o
XD	X_d
XJ	j
XN	X_n
Y	y
Z	z

Subroutine TEMP:

ALX	$\frac{\partial \alpha}{\partial x}$
ALY	$\frac{\partial \alpha}{\partial y}$
ALZ	$\frac{\partial \alpha}{\partial z}$
F	F
FAL	$\frac{\partial F}{\partial \alpha}$
FX	$\frac{\partial F}{\partial x}$
FY	$\frac{\partial F}{\partial y}$
FZ	$\frac{\partial F}{\partial z}$
G	G
GX	$\frac{\partial G}{\partial x}$
GY	$\frac{\partial G}{\partial y}$
GZ	$\frac{\partial G}{\partial z}$
H	H
HX	$\frac{\partial H}{\partial x}$
HY	$\frac{\partial H}{\partial y}$
HZ	$\frac{\partial H}{\partial z}$
KAY	K

Program	Theory
RDX	$\frac{\partial \Phi_{r,d}}{\partial x}$
RDY	$\frac{\partial \Phi_{r,d}}{\partial y}$
S	z
X	θ_g
Y	θ_w
Z	θ_F

Subroutine FLOWS:

F	f(y,z)
FY	$\frac{\partial f}{\partial y}$
FZ	$\frac{\partial f}{\partial z}$
Y	y
YZ	$\frac{dy}{dz}$
Z	z

```
$BATCH
C*************************************************************************
C
C     THIS SMALL-SCALE STEADY-STATE MODEL OF A DEVELOPING FIRE IN*
C     A COMPARTMENT IS BASED ON CONSERVATION LAWS APPLIED TO THE *
C     FUEL, THE ENCLOSURE, THE FIRE PLUME, AND THE UPPER GAS     *
C     LAYER.  SURFACE AND GAS TEMPERATURES, RADIATIVE HEAT FLUX  *
C     TO THE FLOOR, AND FLOW RATES ARE PREDICTED.  THE GEOMETRY  *
C     AND THERMAL PROPERTIES OF THE COMPARTMENT AND THE          *
C     PROPERTIES OF THE FUEL ARE SPECIFIED WITHIN THE PROGRAM.   *
C     NOTE:  THE SIX DOORWAY WIDTHS ARE INPUT FROM AN EXTERNAL   *
C     DATA FILE.                                                 *
C
C*************************************************************************
C
      DIMENSION AMASS(20),BMASS(20),VMASS(20),PYMASS(20),XD(20),
     1XN(20),EG(20),TG(20),TW(20),QR(20),HF(20),FIRE(20),
     2AV(20),TFLR(20),RFDOT(20),QFLR(20),FUEL(20),KE(20),RATIO(20)
      REAL MAX,MB,MA,MPY,MBMAX,MV,L
      REAL MG,INCREM,KW,KG,KFLR,KE
      COMMON DR,HO,RB,MV,ROMEGA,BETA
      COMMON GAMMA,EF,B,MG,D,Z,FF,C,MB,MPY,GG,E,THS,EGA,A,PHI,PI,XJ
      COMMON REF,TA,P,JI,KFLR,MAX,TFLAM
C
C PHYSICAL CONSTANTS:
C     GRAVITY,M/S2
      GRAV=9.8
C     STEFAN-BOLTZMANN CONSTANT, W/(M2-K4)
      SIGMA=5.669E-08
      PI=3.14159
C
C FUEL PARAMETERS:
C
C     AIR TO FUEL MASS RATIO
      R=8.25
C     HEAT OF COMBUSTION, J/KG
      DELH=2.49E+07
C     HEAT OF VOLATILIZATION, J/KG
      DELHV=1.108E+06
C     FUEL SURFACE TEMP, K
      TS=636.
C     DENSITY OF VAPORIZED FUEL, KG/M3
      RHOV=1.92
C     SPECIFIC HEAT OF SOLID FUEL, J/KG-K
      CFUEL=1460.
C     OMEGA FOR PMMA
      OMEGA=0.0968
C
C FIRE PARAMETERS:
C
C     FLAME TEMPERATURE, K
      TFLAM=1400.
C
C HEAT TRANSFER PARAMETERS:
C
```

```
C     FUEL CONVECTIVE HEAT TRANSFER COEFFICIENT, W/M2-K
      HS=2.5
C     WALL AND CEILING CONDUCTANCE, W/M2-K
      KW=5.0
C     FLOOR CONVECTIVE HEAT TRANSFER COEFFICIENT, W/M2-K
      HFLR=10.0
C     TOTAL FLOOR COEFFICIENT, W/M2-K
      KFLR=KW+HFLR
C
C FLOW PARAMETERS:
C
C     DOORWAY FLOW COEFFICIENT
      CO=0.7
C
C FLUID PARAMETERS:
C
C     SPECIFIC HEAT OF AIR AND COMBUSTION PRODUCTS, J/KG-K
      CG=1.046E+03
C     DENSITY OF AIR, KG/M3
      RHO=1.2
C     AIR TEMPERATURE, K
      TA=300.
C     SMOKE CONCENTRATION, MG/L
      CS=4.0
      ROMEGA=OMEGA*RHO/RHOV
C
C COMPARTMENT PARAMETERS:
C
C     HEIGHT, M
      H=0.3
C     WIDTH, M
      W=0.3
C     LENGTH, M
      L=0.56
C     DOORWAY HEIGHT, M
      HO=0.22
C     GUESS AN INITIAL HOT GAS-AIR DENSITY RATIO
      DR=0.5
C
C BEGIN LOOP WHICH WILL BE REPEATED FOR EACH DOOR WIDTH
C
      DO 500 NUMBER=1,6
C     INITIALIZE DIMENSIONLESS TEMPERATURES: GAS, WALL, AND FLOOR
      THGOLD=2.0
      THWOLD=1.5
      THFLRO=1.0
C DOORWAY SPECIFICATIONS:
C     WIDTH, M
      READ (5,91) WO
   91 FORMAT (F5.4)
C
C BEGIN LOOP FOR CHANGING MASS FLOW RATE, KG/S.  NOTE THAT
C THE FUEL INCREMENT INCREASES WITH DOORWAY WIDTH
      INCREM=0.25E-04
      IF (NUMBER .GT. 2) INCREM=0.75E-04
```

```
      IF (NUMBER .GT. 4) INCREM=0.1E-03
      DO 100 JI=1,20
      JII=JI-1
      IF (JI.EQ.1) FUEL(JI)=INCREM
      IF (JI.NE.1) FUEL(JI)=FUEL(JII)+INCREM
C     REINITIALIZE GUESS FOR HOT GAS-AIR DENSITY RATIO
      DR=0.5
C     ENTRAINMENT COEFFICIENT AS A FUNCTION OF FUEL
      KE(JI)=0.1+0.5*(FUEL(JI)*1000.)
C     BETA (FOR PMMA)
      BETA=8.2*HO*KE(JI)**0.8/FUEL(JI)**0.4
C     PARAMETER TO MAKE FLOWS DIMENSIONLESS
      MAX=(2./3.)*CO*RHO*SQRT(2.*GRAV)*WO*HO**1.5
C     DIMENSIONLESS FUEL FLOW
      MV=FUEL(JI)/MAX
C
C DETERMINE DIMENSIONLESS DOORWAY AND COMPARTMENT NEUTRAL
C PLANE HEIGHTS FROM FLOW EQUATIONS
   52 CONTINUE
      CALL FLOWS (Y)
C DETERMINATION OF FLOW RATES BASED ON NEUTRAL PLANE HEIGHTS:
C     COMPARTMENTAL NEUTRAL PLANE HEIGHT, M
      XD(JI)=Z*HO
C     DOORWAY NEUTRAL PLANE HEIGHT, M
      XN(JI)=Y*HO
C     DETERMINE F24:  SHAPE FACTOR FOR RADIATION TO THE FLOOR
      XDA=XD(JI)
      CALL SHAPE (XDA,W,L,F24)
C
C     AIR FLOW--DIMENSIONLESS
      MA=SQRT(DR*(1.-DR))*(1.-Y)**1.5-MV
C
C DETERMINE WHETHER ALL AVAILABLE FUEL IS BEING BURNED:
C     MAXIMUM AMOUNT OF FUEL THAT MAY BE BURNED FOR THE
C     CALCULATED AIR FLOW
      MBMAX=MA/R
C IS ALL AVAILABLE FUEL BURNED---
      IF (MV.LE.MBMAX) GO TO 20
C     IF NOT ALL BURNED, THEN
      MB=MBMAX
C     MASS PYROLYZED--DIMENSIONLESS
      MPY=MV-MB
      GO TO 30
C     IF IT IS ALL BURNED, THEN:
   20 MB=MV
      MPY=0.0
C     GAS FLOW
   30 MG=MA+MV
C*********************************************************************
C                                                                    *
C THIS SECTION WILL DETERMINE HEAT TRANSFER PARAMETERS,              *
C TEMPERATURES OF GAS, WALL, AND FLOOR, AND WILL PREPARE VALUES      *
C FOR OUTPUT                                                         *
C                                                                    *
C*********************************************************************
```

```
C
C  DIMENSIONALIZE MASS FLOWS, KG/S
C     AIR FLOW
      AMASS(JI)=MA*MAX
C     MASS BURNED
      BMASS(JI)=MB*MAX
C     MASS OF FUEL VAPORIZED
      VMASS(JI)=MV*MAX
C     MASS OF FUEL PYROLYZED, BUT NOT BURNED
      PYMASS(JI)=MPY*MAX
C      AIR TO FUEL RATIO
       RATIO(JI)=MA/MV
C
C CALCULATE THERMAL PROPERTIES:
C     ENERGY RELEASE RATE, KW
      FIRE(JI)=BMASS(JI)*DELH/1.E+03
C     HEAT TRANSFER COEFFICIENT, W/(M2-K)
      HW=14.4*(FIRE(JI)**0.333)
C     DIMENSIONLESS FUEL SURFACE TEMPERATURE
      THS=TS/TA
C
C     KAPPA AS A FUNCTION OF THE FLOW RATES
      KG=0.3+((4.64*MB)/(MA+0.6*MB))
C     GAS EMISSIVITY
      EG(JI)=1.0-EXP(-(KG+0.47*CS)*(H-XD(JI)))
      EGA=EG(JI)
C     FLAME HEIGHT, M
      HF(JI)=16.2*((BMASS(JI)**2*(R+(OMEGA*RHO/RHOV))**2*OMEGA)/
     1(RHO**2*GRAV*(1.-OMEGA)**5))**0.2
C     FLAME HEIGHT CAN BE NO GREATER THAN COMPARTMENTAL
C     NEUTRAL PLANE HEIGHT, SO
      IF (HF(JI).GT.XD(JI)) HF(JI)=XD(JI)
C     FLAME EMISSIVITY
      EF=1.0-EXP(-1.3*HF(JI))
C     FLOOR FACTOR TO REDUCE CONTRIBUTION FROM THE FLOOR
      FFLR=1.0-W/SQRT(W**2+4.*XD(JI)**2)
C
C CALCULATE PARAMETERS AND THE COEFFICIENTS OF THE TERMS
C USED IN DETERMINATION OF TEMPERATURES
C     FLOOR AREA, M2
      AF=W*L
C     WALL AREA OF UPPER GAS LAYER, M2
      AW=W*L+2.0*(H-XD(JI))*(W+L)
      GAMMA=AF/AW
      REF=SIGMA*TA**3
      XJ=HS/REF
      A=HW/REF
      B=KW/REF
      C=(MAX*DELH)/(AW*REF*TA)
      D=(CG*MAX)/(AW*REF)
      E=CFUEL*MAX/(AW*REF)
      FF=HO/SQRT(AW)
      GG=DELHV*MAX/(AW*REF*TA)
      P=HO*WO/AW
C
```

```
C CALCULATE TEMPERATURES:
C     START CALCULATION WITH PREVIOUSLY DETERMINED TEMPS
C     TO REDUCE TIME REQUIRED FOR COMPUTATION
      THG=THGOLD
      THW=THWOLD
      THFLR=THFLRO
      CALL TEMP (THG,THW,THFLR,F,G,ALPHA,RD,RW,RF,F24,FFLR)
      THGOLD=THG
      THWOLD=THW
      THFLRO=THFLR
C
C DIMENSIONALIZE VARIABLES FOR OUTPUT:
C     FIRE AREA,M2
      AV(JI)=ALPHA*AW
C     RD CORRECTED TO YIELD SENSOR FLUX
      RD=RD-1.+THFLR**4
C     RADIATION TO THE FLOOR
      QR(JI)=1.E-04*SIGMA*TA**4*RD*F24
C     GAS TEMPERATURE, C
      TG(JI)=THG*TA-273.
C     WALL TEMPERATURE, C
      TW(JI)=THW*TA-273.
C     FLOOR TEMPERATURE, C
      TFLR(JI)=THFLR*TA-273.
C     FIRE RADIATIVE FLUX, W/CM2
      QFIRE=1.E-04*SIGMA*TA**4*RF
C     RADIANT ENERGY LOSS BY FIRE, KW
      RFDOT(JI)=QFIRE*(2.*HF(JI)*SQRT(PI*AV(JI)))
C     HEAT FLUX TO SENSOR
      QFLR(JI)=QR(JI)+0.1*(RFDOT(JI)/AF)
C     WALL RADIATIVE FLUX, W/CM2
      QWALL=1.0E-04*SIGMA*TA**4*RW
C
C REITERATE FLOW WITH NEW GAS TEMPERATURE:
C     COMPUTE NEW HOT-AIR DENSITY RATIO
      DRNEW=1./THG
      IF (ABS((DRNEW-DR)/DR)-.1) 51,51,50
   50 DR=DRNEW
      IF (DR.GE.1.) GO TO 55
      IF (DR.LE.0.) GO TO 55
      GO TO 52
   55 WRITE(6,22)
   22 FORMAT (/,20X,'DR DOES NOT CONVERGE')
   51 CONTINUE
C
  100 CONTINUE
  400 CONTINUE
C
C***********************************************************************
C
C***********************************************************************
C
      WRITE (6,1)
    1 FORMAT (1H1,///,8X,'NUMBER',5X,'AMASS',6X,'BMASS',6X,'VMASS',6X,
     2'PYMASS',7X,'XD',9X,'XN',9X,'HF',8X,'FIRE',/,21X,3('KG/S',7X),'KG
```

```
      2/S',6X,3('M',10X),'KW')
       DO 11 IJ=1,20
   11 WRITE (6,2) IJ, AMASS(IJ),BMASS(IJ),VMASS(IJ),PYMASS(IJ),XD(IJ),
      1XN(IJ),HF(IJ),FIRE(IJ)
    2 FORMAT (1H0,8X,I4,3X,8(2X,E9.4))
       WRITE (6,3)
    3 FORMAT (1H1,///,9X, 'NUMBER',2X,'EG',8X,'TG',8X,'TW',5X,'TFLR',
      18X,'QR',6X,
      1' AV  ',7X, 'RFDOT',5X,'QFLR ',6X,'FUEL',6X,'MA/MV',
      1/,27X,'C',9X,
      1'C',9X,'C',7X,'W/CM-2',4X,'M-2',10X,'KW',5X,'W/CM-2',6X,'KG/S')
       DO 12 IN=1,20
   12 WRITE(6,4) IN, EG(IN),TG(IN),TW(IN),TFLR(IN),QR(IN),AV(IN),
      1RFDOT(IN),QFLR(IN), FUEL(IN),RATIO(IN)
    4 FORMAT (1H0, 7X,I4,10(1X,E9.4))
       WRITE (6,85) CS,WO,KW,L,W
   85 FORMAT (1H0,///,20X,'CS=',F5.2,2X,'WO=',F5.4,2X, 2X,'KW=',
      1F6.2,5X, F5.2,'X',F5.2,2X,'ROOM')
  500 CONTINUE
       STOP
       END
       SUBROUTINE TEMP (X,Y,Z,F,G,ALPHA,RD,RW,RF,F24,FFLR)
       REAL MAX,MPY,MV,MG,MB
       REAL KAY,KFLR
       COMMON DR,HO,RB,MV,ROMEGA,BETA
       COMMON GAMMA,EF,B,MG,D,S,FF,C,MB,MPY,GG,E,THS,EG,A,PHI,PI,XJ
       COMMON REF,TA,P,JI,KFLR,MAX,TFLAM
C
C
C      INITIAL VALUES
       N=0
C      NOTE: X IS THETA GAS, Y IS THETA WALL, AND Z IS THETA FLOOR
C*****************************************************************
C                                                                *
C      THIS SUBROUTINE UTILIZES A THREE VARIABLE  NEWTON-RAPHSON *
C      METHOD TO CALCULATE THE WALL, GAS, AND FLOOR TEMPERATURES *
C      USING THE THREE ALGEBRAIC EQUATIONS F,G, AND H SET EQUAL  *
C      TO ZERO (SEE BELOW)                                       *
C                                                                *
C******************************************************************
    5 N=N+1
       IF(N.EQ.20)GO TO 11
       KAY=F24/(KFLR/REF)
C      FLUX THRU THE BOTTOM OF THE HOT GAS LAYER
C      FLAME TEMPERATURE,K
C      DIMENSIONLESS FLAME TEMPERATURE
       THFLAM=TFLAM/TA
       RD=EG*X**4+(1.-EG)*Y**4-Z**4
       RW=EG*  X**4+GAMMA*(1.-EG)*Z**4-(1.-(1.-GAMMA)*
      1(1.-EG))*Y**4
C      RADIATION FROM THE FLAME
       RF=EF*THFLAM**4
C      ALPHA IS THE DIMENSIONLESS FUEL AREA
       ALPHA=MV*(E*(THS-1.)+GG)/(F24*(1.-EF)*(EG*X**4+(1.-EG)*Y**4
      *-1.)+EF*THFLAM**4+(1.-EF)*FFLR*Z**4+XJ*(THFLAM-THS)-THS**4)
```

```
      IF (ALPHA.GE.0.) GO TO 22
      WRITE (6,21)
   21 FORMAT (1H , 20X,'ALPHA IS NEGATIVE')
      WRITE (6,7) N,ALPHA,RD,Z,X,Y,JI
    7 FORMAT (1H , 'N=',I5, 'ALPHA=',F9.3, 'RD=',F9.3, 'Z=',F9.3, 'X=
     -', F9.3, 'Y=', F9.3,/,20X,'NUMBER=',I3)
      ALPHA=0.01
C
C CALCULATE DERIVATIVES NECESSARY FOR NEWTON-RAPHSON METHOD
   22 RDX=4.*EG*X**3
      RDY=4.*(1.-EG)*Y**3
      ALX=(-(ALPHA**2)/(MV*(E*(THS-1.)+GG)))*((1.-EF)*RDX*F24)
      ALY=(-(ALPHA**2)/(MV*(E*(THS-1.)+GG)))*((1.-EF)*RDY*F24)
      ALZ=(-(ALPHA**2)*4.*(1.-EF)*FFLR*Z**3)/(MV*(E*(THS-1.)+GG))
      GX=4.*EG*X**3+A
      GY=-4.*(1.-(1.-GAMMA)*(1.-EG))*Y**3-B-A
      GZ=4.*GAMMA*(1.-EG)*Z**3
      FAL=-EF*F24*(EG*X**4+(1.-EG)*Y**4-1.)+
     *SQRT(PI)*S*FF*RF*ALPHA**(-0.5)
      FX=4.*EG*X**3*(GAMMA-EF*ALPHA*F24)+MG*D+FAL*ALX+4.*P*EG*X**3
      FY=4.*(1.-EG)*Y**3*(GAMMA-EF*ALPHA*F24)+B+FAL*ALY+4.*P
     **(1.-EG)*Y**3
      FZ=-4.*GAMMA*Z**3+FAL*ALZ
      HX=-4.*KAY*EG*X**3
      HY=-4.*KAY*(1.-EG)*Y**3
      HZ=1.+4.*KAY*Z**3
      EDD=E-D
      XYY=X-Y
      F=GAMMA*RD-EF*ALPHA*F24*(RD+Z**4-1.)+B*(Y-1.)+MG*D*(X-1.)
     * +2.*SQRT(PI)*S*FF*RF*SQRT(ALPHA)-C*MB+MPY*(GG+EDD*(THS-1.))
     * +P*(EG*X**4+(1.-EG)*Y**4)
      G=EG*X**4+GAMMA*(1.-EG)*Z**4-(1.-(1.-GAMMA)*(1.-EG))
     **Y**4-B*(Y-1.)+(A*(XYY))
      H=Z-1.-RD*KAY
      DELTA=FX*(GY*HZ-HY*GZ)-FY*(GX*HZ-HX*GZ)+FZ*(GX*HY-HX*GY)
      DX=(-F*(GY*HZ-HY*GZ)-FY*(-G*HZ+H*GZ)+FZ*(-G*HY+H*GY))/DELTA
      DY=(FX*(-G*HZ+H*GZ)+F*(GX*HZ-HX*GZ)+FZ*(-H*GX+G*HX))/DELTA
      DZ=(FX*(-H*GY+G*HY)-FY*(-H*GX+G*HX)-F*(GX*HY-HX*GY))/DELTA
      X=X+DX
      Y=Y+DY
      Z=Z+DZ
      TOLX=ABS(DX/X)
      TOLY=ABS(DY/Y)
      TOLZ=ABS(DZ/Z)
      IF(TOLX-0.001)10,10,5
   10 IF(TOLY-0.001)12,12,5
   12 IF (TOLZ-0.001) 13,13,5
   11 WRITE(6,1)
    1 FORMAT (1H0,5X,'ITERATION FOR X,Y DOES NOT CONVERGE')
   13 RETURN
      END
      SUBROUTINE FLOWS(Y)
C*************************************************************
C       THIS SUBROUTINE CALCULATES THE DOORWAY
C       AND COMPARTMENTAL NEUTRAL PLANE HEIGHTS
```

```
C      (Y,Z) BY SETTING THE FLOW EQUATION F
C      EQUAL TO ZERO
C*******************************************************
      REAL MV,KFLR
      COMMON DR,HO,RB,MV,ROMEGA,BETA
      COMMON GAMMA,EF,B,MG,D,Z,FF,C,MB,MFY,GG,E,THS,EG,A,PHI,PI,XJ
      COMMON REF,TA,P,JI,KFLR,MAX,TFLAM
C
C     GUESS INITIAL VALUE
      Z=0.5
      N=1
C
C     CALCULATE Z
    5 N=N+1
      IF (N.EQ.20) GO TO 8
      Y=1.-MV**(2./3.)*(1.+ROMEGA*(BETA*Z+1.)**2.5)**(2./3.)/
     1  (DR*(1.-DR))**(1./3.)
      F=(Y-Z)*(Y+Z/2.)**2-((ROMEGA**2*MV**2)/(1.-DR))*(BETA*Z+1.)**5
      FZ=(Y-Z)*(Y+Z/2.)-(Y+Z/2.)**2-5.*BETA*ROMEGA**2*MV**2*
     1    (BETA*Z+1.)**4/(1.-DR)
      FY=2.*(Y-Z)*(Y+Z/2.)+(Y+Z/2.)**2
      YZ=-(5./3.)*ROMEGA*BETA*MV**(2./3.)*(BETA*Z+1.)**1.5/
     1     (DR*(1.-DR)*(1.+ROMEGA*(BETA*Z+1.)**2.5))**(1./3.)
      DF=FZ+FY*YZ
      DZ=-F/DF
      Z=Z+DZ
      IF(Z .LT. 0.) Z=.5*(Z-DZ)
      TOL=ABS(DZ/Z)
      IF  (TOL-0.0005) 10,10,5
    8 WRITE(6,9) JI
    9 FORMAT(1H0,5X,'NEWT DOES NOT CONVERGE',5X,'NUMBER=',I3)
   10 RETURN
      END
      SUBROUTINE SHAPE (XD,W,L,F24)
C*********************************************************************
C     THIS SUBROUTINE CALCULATES F24---
C     A VIEW FACTOR FOR THE RADIATION TO THE FLOOR
C*********************************************************************
      REAL L
      PI=3.14159
      X=L/XD
      Y=W/XD
      PART1=ALOG((((1+X**2)*(1+Y**2)/(1+X**2+Y**2))**0.5)
      PART2=Y*SQRT(1+X**2)*ATAN(Y/SQRT(1+X**2))
      PART3=X*SQRT(1+Y**2)*ATAN(X/SQRT(1+Y**2))
      PART4=-Y*ATAN(Y)-X*ATAN(X)
      F24=(2/(PI*X*Y))*(PART1+PART2+PART3+PART4)
      RETURN
      END
$BEND
```

NUMBER	AMASS KG/S	BMASS KG/S	VMASS KG/S	PYMASS KG /S	XD M	XN M	HF M	FIRE KW
1	.4262E-03	.2500E-04	.2500E-04	.0000E+00	.8637E-01	.1175E+00	.8637E-01	.6225E+00
2	.5725E-03	.5000E-04	.5000E-04	.0000E+00	.8753E-01	.1136E+00	.8753E-01	.1245E+01
3	.6242E-03	.7500E-04	.7500E-04	.0000E+00	.8236E-01	.1078E+00	.8236E-01	.1867E+01
4	.6312E-03	.7651E-04	.1000E-03	.2349E-04	.7574E-01	.1044E+00	.7574E-01	.1905E+01
5	.6350E-03	.7696E-04	.1250E-03	.4804E-04	.6998E-01	.1013E+00	.6998E-01	.1916E+01
6	.6349E-03	.7695E-04	.1500E-03	.7305E-04	.6493E-01	.9877E-01	.6493E-01	.1916E+01
7	.6322E-03	.7664E-04	.1750E-03	.9836E-04	.6045E-01	.9648E-01	.6045E-01	.1908E+01
8	.6111E-03	.7407E-04	.2000E-03	.1259E-03	.5568E-01	.9557E-01	.5568E-01	.1844E+01
9	.6019E-03	.7296E-04	.2250E-03	.1520E-03	.5196E-01	.9379E-01	.5196E-01	.1817E+01
10	.5915E-03	.7169E-04	.2500E-03	.1783E-03	.4858E-01	.9211E-01	.4858E-01	.1785E+01
11	.5788E-03	.7016E-04	.2750E-03	.2048E-03	.4547E-01	.9060E-01	.4547E-01	.1747E+01
12	.5652E-03	.6851E-04	.3000E-03	.2315E-03	.4261E-01	.8911E-01	.4261E-01	.1706E+01
13	.5505E-03	.6672E-04	.3250E-03	.2583E-03	.3994E-01	.8766E-01	.3994E-01	.1661E+01
14	.5338E-03	.6471E-04	.3500E-03	.2853E-03	.3744E-01	.8628E-01	.3744E-01	.1611E+01
15	.5155E-03	.6249E-04	.3750E-03	.3125E-03	.3505E-01	.8489E-01	.3505E-01	.1556E+01
16	.4932E-03	.6003E-04	.4000E-03	.3400E-03	.3276E-01	.8346E-01	.3276E-01	.1495E+01
17	.3878E-03	.4701E-04	.4250E-03	.3780E-03	.2717E-01	.8065E-01	.2717E-01	.1171E+01
18	.2724E-04	.3302E-05	.4500E-03	.4467E-03	.1562E-05	.2821E-01	.1562E-05	.8222E-01
19	.4038E-03	.4895E-04	.4750E-03	.4261E-03	.2558E-01	.7836E-01	.2558E-01	.1219E+01
20	.4205E-03	.5096E-04	.5000E-03	.4490E-03	.2519E-01	.5701E-01	.2519E-01	.1269E+01

NUMBER	EG	TG C	TW C	TFLR C	QR W/CM-2	AV M-2	RFDOT KW	QFLR W/CM-2	FUEL KG/S	MA/MV
1	.4066E+00	.1062E+03	.8523E+02	.4647E+02	.3792E-01	.2471E-02	.3520E-01	.5887E-01	.2500E-04	.1705E+02
2	.4202E+00	.2057E+03	.1687E+03	.9257E+02	.1349E+00	.4598E-02	.4928E-01	.1642E+00	.5000E-04	.1145E+02
3	.4444E+00	.2980E+03	.2536E+03	.1638E+03	.3138E+00	.6737E-02	.5299E-01	.3454E+00	.7500E-04	.8322E+01
4	.4547E+00	.2937E+03	.2507E+03	.1632E+03	.3153E+00	.9922E-02	.5461E-01	.3478E+00	.1000E-03	.6312E+01
5	.4631E+00	.2876E+03	.2459E+03	.1604E+03	.3106E+00	.1371E-01	.5500E-01	.3433E+00	.1250E-03	.5080E+01
6	.4704E+00	.2810E+03	.2406E+03	.1570E+03	.3034E+00	.1817E-01	.5469E-01	.3360E+00	.1500E-03	.4232E+01
7	.4768E+00	.2742E+03	.2349E+03	.1530E+03	.2944E+00	.2343E-01	.5398E-01	.3266E+00	.1750E-03	.3613E+01
8	.4835E+00	.2601E+03	.2223E+03	.1430E+03	.2698E+00	.3063E-01	.5252E-01	.3001E+00	.2000E-03	.3056E+01
9	.4887E+00	.2508E+03	.2142E+03	.1369E+03	.2536E+00	.3862E-01	.5150E-01	.2843E+00	.2250E-03	.2675E+01
10	.4933E+00	.2409E+03	.2055E+03	.1302E+03	.2371E+00	.4841E-01	.5050E-01	.2671E+00	.2500E-03	.2366E+01
11	.4976E+00	.2297E+03	.1957E+03	.1225E+03	.2181E+00	.6066E-01	.4963E-01	.2477E+00	.2750E-03	.2105E+01
12	.5015E+00	.2176E+03	.1850E+03	.1144E+03	.1982E+00	.7626E-01	.4995E-01	.2273E+00	.3000E-03	.1884E+01
13	.5050E+00	.2044E+03	.1734E+03	.1057E+03	.1771E+00	.9677E-01	.4853E-01	.2059E+00	.3250E-03	.1694E+01
14	.5084E+00	.1891E+03	.1601E+03	.9602E+02	.1528E+00	.1253E+00	.4960E-01	.1818E+00	.3500E-03	.1525E+01
15	.5115E+00	.1713E+03	.1446E+03	.8529E+02	.1274E+00	.1676E+00	.4935E-01	.1568E+00	.3750E-03	.1375E+01
16	.5146E+00	.1491E+03	.1257E+03	.7296E+02	.9901E-01	.2384E+00	.5150E-01	.1297E+00	.4000E-03	.1238E+01
17	.5218E+00	.9209E+02	.6213E+02	.1577E+01	.2258E+00	.3003E+00	.3989E-01	.2495E+00	.4250E-03	.9125E+00
18	.5557E+00	.1478E+03	.7167E+02	.7034E+01	.4101E-01	.6940E-02	.1903E-10	.4101E-01	.4500E-03	.6054E-01
19	.5239E+00	.2236E+02	.1004E+02	.3509E+02	.1344E+00	.5344E+00	.4721E-01	.1625E+00	.4750E-03	.8501E+00
20	.5244E+00	.1482E+04	.2110E+04	.1503E+04	.5195E+02	.1567E-02	.2481E-02	.5195E+02	.5000E-03	.8409E+00

CS= 4.00 WO=.0150 KW= 5.00 0.56X 0.30 ROOM

NUMBER	AMASS KG/S	BMASS KG/S	VMASS KG/S	PYMASS KG /S	XD M	XN M	HF M	FIRE KW
1	.7724E-03	.2500E-04	.2500E-04	.0000E+00	.1123E+00	.1290E+00	.1123E+00	.6225E+00
2	.9357E-03	.5000E-04	.5000E-04	.0000E+00	.1092E+00	.1256E+00	.1092E+00	.1245E+01
3	.1065E-02	.7500E-04	.7500E-04	.0000E+00	.1052E+00	.1213E+00	.1052E+00	.1867E+01
4	.1138E-02	.1000E-03	.1000E-03	.0000E+00	.9956E-01	.1165E+00	.9956E-01	.2490E+01
5	.1186E-02	.1250E-03	.1250E-03	.0000E+00	.9393E-01	.1120E+00	.9393E-01	.3112E+01
6	.1218E-02	.1476E-03	.1500E-03	.2363E-05	.8859E-01	.1081E+00	.8859E-01	.3676E+01
7	.1242E-02	.1506E-03	.1750E-03	.2444E-04	.8373E-01	.1054E+00	.8373E-01	.3749E+01
8	.1261E-02	.1528E-03	.2000E-03	.4719E-04	.7930E-01	.1030E+00	.7930E-01	.3805E+01
9	.1273E-02	.1543E-03	.2250E-03	.7067E-04	.7527E-01	.1010E+00	.7527E-01	.3843E+01
10	.1285E-02	.1557E-03	.2500E-03	.9430E-04	.7157E-01	.9907E-01	.7157E-01	.3877E+01
11	.1291E-02	.1565E-03	.2750E-03	.1185E-03	.6817E-01	.9742E-01	.6817E-01	.3897E+01
12	.1295E-02	.1569E-03	.3000E-03	.1431E-03	.6504E-01	.9599E-01	.6504E-01	.3907E+01
13	.1297E-02	.1572E-03	.3250E-03	.1678E-03	.6214E-01	.9460E-01	.6214E-01	.3915E+01
14	.1296E-02	.1571E-03	.3500E-03	.1929E-03	.5946E-01	.9342E-01	.5946E-01	.3912E+01
15	.1295E-02	.1570E-03	.3750E-03	.2180E-03	.5696E-01	.9225E-01	.5696E-01	.3910E+01
16	.1293E-02	.1567E-03	.4000E-03	.2433E-03	.5463E-01	.9119E-01	.5463E-01	.3902E+01
17	.1288E-02	.1561E-03	.4250E-03	.2689E-03	.5245E-01	.9024E-01	.5245E-01	.3887E+01
18	.1282E-02	.1554E-03	.4500E-03	.2946E-03	.5041E-01	.8934E-01	.5041E-01	.3871E+01
19	.1276E-02	.1547E-03	.4750E-03	.3203E-03	.4850E-01	.8850E-01	.4850E-01	.3851E+01
20	.1270E-02	.1539E-03	.5000E-03	.3461E-03	.4670E-01	.8767E-01	.4670E-01	.3832E+01

NUMBER	EG	TG C	TW C	TFLR C	QR W/CM-2	AV M-2	RFDOT KW	QFLR W/CM-2	FUEL KG/S	MA/MV
1	.3540E+00	.6302E+02	.5261E+02	.3357E+02	.1231E-01	.1784E-02	.4972E-01	.4191E-01	.2500E-04	.3090E+02
2	.3698E+00	.1637E+03	.1319E+03	.6594E+02	.7594E-01	.3594E-02	.6689E-01	.1157E+00	.5000E-04	.1871E+02
3	.3848E+00	.2500E+03	.2066E+03	.1157E+03	.1841E+00	.5381E-02	.7615E-01	.2294E+00	.7500E-04	.1420E+02
4	.4023E+00	.3293E+03	.2801E+03	.1825E+03	.3573E+00	.7083E-02	.7853E-01	.4040E+00	.1000E-03	.1138E+02
5	.4196E+00	.4040E+03	.3533E+03	.2606E+03	.6157E+00	.8418E-02	.7648E-01	.6612E+00	.1250E-03	.9490E+01
6	.4354E+00	.4697E+03	.4203E+03	.3367E+03	.9489E+00	.9311E-02	.7179E-01	.9917E+00	.1500E-03	.8120E+01
7	.4428E+30	.4730E+03	.4249E+03	.3436E+03	.9946E+00	.1121E-01	.7059E-01	.1037E+01	.1750E-03	.7098E+01
8	.4494E+00	.4753E+03	.4282E+03	.3490E+03	.1033E+01	.1323E-01	.6897E-01	.1074E+01	.2000E-03	.6303E+01
9	.4554E+00	.4760E+03	.4298E+03	.3523E+03	.1061E+01	.1538E-01	.6717E-01	.1101E+01	.2250E-03	.5659E+01
10	.4608E+00	.4766E+03	.4313E+03	.3553E+03	.1087E+01	.1763E-01	.6518E-01	.1126E+01	.2500E-03	.5138E+01
11	.4658E+00	.4759E+03	.4313E+03	.3565E+03	.1103E+01	.2004E-01	.6319E-01	.1141E+01	.2750E-03	.4696E+01
12	.4703E+00	.4741E+03	.4301E+03	.3564E+03	.1111E+01	.2264E-01	.6126E-01	.1148E+01	.3000E-03	.4315E+01
13	.4744E+00	.4722E+03	.4287E+03	.3559E+03	.1117E+01	.2539E-01	.5933E-01	.1152E+01	.3250E-03	.3991E+01
14	.4782E+00	.4690E+03	.4261E+03	.3539E+03	.1113E+01	.2839E-01	.5753E-01	.1148E+01	.3500E-03	.3703E+01
15	.4817E+00	.4659E+03	.4235E+03	.3518E+03	.1109E+01	.3155E-01	.5575E-01	.1142E+01	.3750E-03	.3455E+01
16	.4850E+00	.4621E+03	.4201E+03	.3489E+03	.1099E+01	.3499E-01	.5408E-01	.1131E+01	.4000E-03	.3232E+01
17	.4880E+00	.4576E+03	.4159E+03	.3450E+03	.1083E+01	.3873E-01	.5253E-01	.1114E+01	.4250E-03	.3030E+01
18	.4908E+00	.4528E+03	.4114E+03	.3407E+03	.1065E+01	.4278E-01	.5106E-01	.1095E+01	.4500E-03	.2850E+01
19	.4935E+00	.4475E+03	.4064E+03	.3359E+03	.1043E+01	.4719E-01	.4969E-01	.1073E+01	.4750E-03	.2686E+01
20	.4959E+00	.4422E+03	.4014E+03	.3310E+03	.1021E+01	.5193E-01	.4839E-01	.1050E+01	.5000E-03	.2539E+01

CS= 4.00 WO=.0300 KW= 5.00 0.56X 0.30 ROOM

NUMBER	AMASS KG/S	BMASS KG/S	VMASS KG/S	PYMASS KG /S	XD M	XN M	HF M	FIRE KW
1	.1868E-02	.7500E-04	.7500E-04	.0000E+00	.1350E+00	.1419E+00	.1350E+00	.1067E+01
2	.2423E-02	.1500E-03	.1500E-03	.0000E+00	.1212E+00	.1301E+00	.1212E+00	.3735E+01
3	.2750E-02	.2250E-03	.2250E-03	.0000E+00	.1077E+00	.1188E+00	.1077E+00	.5602E+01
4	.2944E-02	.3000E-03	.3000E-03	.0000E+00	.9593E-01	.1099E+00	.9593E-01	.7470E+01
5	.3057E-02	.3705E-03	.3750E-03	.4472E-05	.8607E-01	.1028E+00	.8607E-01	.9226E+01
6	.3159E-02	.3829E-03	.4500E-03	.6710E-04	.7830E-01	.9836E-01	.7830E-01	.9534E+01
7	.3236E-02	.3923E-03	.5250E-03	.1327E-03	.7173E-01	.9494E-01	.7173E-01	.9767E+01
8	.3284E-02	.3981E-03	.6000E-03	.2019E-03	.6610E-01	.9210E-01	.6610E-01	.9912E+01
9	.3316E-02	.4019E-03	.6750E-03	.2731E-03	.6122E-01	.8983E-01	.6122E-01	.1001E+02
10	.3334E-02	.4041E-03	.7500E-03	.3459E-03	.5695E-01	.8793E-01	.5695E-01	.1006E+02
11	.3341E-02	.4050E-03	.8250E-03	.4200E-03	.5320E-01	.8634E-01	.5320E-01	.1008E+02
12	.3341E-02	.4050E-03	.9000E-03	.4950E-03	.4986E-01	.8496E-01	.4986E-01	.1008E+02
13	.3335E-02	.4042E-03	.9750E-03	.5708E-03	.4689E-01	.8376E-01	.4689E-01	.1006E+02
14	.3324E-02	.4029E-03	.1050E-02	.6471E-03	.4422E-01	.8269E-01	.4422E-01	.1003E+02
15	.3309E-02	.4011E-03	.1125E-02	.7239E-03	.4180E-01	.8173E-01	.4180E-01	.9986E+01
16	.3291E-02	.3989E-03	.1200E-02	.8011E-03	.3961E-01	.8086E-01	.3961E-01	.9933E+01
17	.3271E-02	.3965E-03	.1275E-02	.8785E-03	.3761E-01	.8006E-01	.3761E-01	.9872E+01
18	.3249E-02	.3938E-03	.1350E-02	.9562E-03	.3578E-01	.7933E-01	.3578E-01	.9805E+01
19	.3223E-02	.3907E-03	.1425E-02	.1034E-02	.3410E-01	.7869E-01	.3410E-01	.9728E+01
20	.3200E-02	.3879E-03	.1500E-02	.1112E-02	.3255E-01	.7801E-01	.3255E-01	.9659E+01

NUMBER	EG	TG C	TW C	TFLR C	QR W/CM-2	AV M-2	RFDOT KW	QFLR W/CM-2	FUEL KG/S	MA/MV
1	.3227E+00	.1754E+03	.1414E+03	.6681E+02	.7565E-01	.4208E-02	.1089E+00	.1405E+00	.7500E-04	.2491E+02
2	.3555E+00	.3644E+03	.3094E+03	.2024E+03	.4017E+00	.8452E-02	.1255E+00	.4763E+00	.1500E-03	.1615E+02
3	.3867E+00	.5252E+03	.4705E+03	.3849E+03	.1150E+01	.1095E-01	.1136E+00	.1218E+01	.2250E-03	.1222E+02
4	.4148E+00	.6759E+03	.6295E+03	.5677E+03	.2582E+01	.1068E-01	.8974E-01	.2635E+01	.3000E-03	.9814E+01
5	.4393E+00	.8038E+03	.7656E+03	.7188E+03	.4653E+01	.9397E-02	.6818E-01	.4693E+01	.3750E-03	.8152E+01
6	.4509E+00	.8154E+03	.7795E+03	.7355E+03	.5068E+01	.1098E-01	.6130E-01	.5105E+01	.4500E-03	.7020E+01
7	.4606E+00	.8222E+03	.7880E+03	.7460E+03	.5382E+01	.1262E-01	.5539E-01	.5415E+01	.5250E-03	.6164E+01
8	.4688E+00	.8238E+03	.7907E+03	.7501E+03	.5574E+01	.1441E-01	.5044E-01	.5604E+01	.6000E-03	.5474E+01
9	.4757E+00	.8223E+03	.7901E+03	.7505E+03	.5684E+01	.1634E-01	.4621E-01	.5711E+01	.6750E-03	.4913E+01
10	.4817E+00	.8182E+03	.7866E+03	.7477E+03	.5721E+01	.1844E-01	.4260E-01	.5746E+01	.7500E-03	.4445E+01
11	.4870E+00	.8122E+03	.7810E+03	.7426E+03	.5700E+01	.2073E-01	.3951E-01	.5723E+01	.8250E-03	.4050E+01
12	.4916E+00	.8046E+03	.7738E+03	.7356E+03	.5633E+01	.2324E-01	.3683E-01	.5655E+01	.9000E-03	.3712E+01
13	.4957E+00	.7959E+03	.7652E+03	.7271E+03	.5529E+01	.2599E-01	.3451E-01	.5550E+01	.9750E-03	.3420E+01
14	.4993E+00	.7861E+03	.7556E+03	.7174E+03	.5397E+01	.2901E-01	.3248E-01	.5417E+01	.1050E-02	.3165E+01
15	.5025E+00	.7756E+03	.7451E+03	.7068E+03	.5243E+01	.3233E-01	.3069E-01	.5262E+01	.1125E-02	.2941E+01
16	.5055E+00	.7644E+03	.7339E+03	.6953E+03	.5072E+01	.3598E-01	.2912E-01	.5089E+01	.1200E-02	.2743E+01
17	.5081E+00	.7526E+03	.7221E+03	.6831E+03	.4889E+01	.3998E-01	.2771E-01	.4905E+01	.1275E-02	.2565E+01
18	.5106E+00	.7403E+03	.7097E+03	.6703E+03	.4693E+01	.4457E-01	.2651E-01	.4709E+01	.1350E-02	.2406E+01
19	.5128E+00	.7273E+03	.6965E+03	.6567E+03	.4489E+01	.4949E-01	.2540E-01	.4504E+01	.1425E-02	.2262E+01
20	.5148E+00	.7146E+03	.6837E+03	.6433E+03	.4292E+01	.5490E-01	.2440E-01	.4307E+01	.1500E-02	.2134E+01

CS= 4.00 WO=.0770 KW= 5.00 0.56X 0.30 ROOM

NUMBER	AMASS KG/S	BMASS KG/S	VMASS KG/S	PYMASS KG /S	XD M	XN M	HF M	FIRE KW
1	.2229E-02	.7500E-04	.7500E-04	.0000E+00	.1459E+00	.1505E+00	.1459E+00	.1867E+01
2	.3070E-02	.1500E-03	.1500E-03	.0000E+00	.1347E+00	.1401E+00	.1347E+00	.3735E+01
3	.3610E-02	.2250E-03	.2250E-03	.0000E+00	.1217E+00	.1292E+00	.1217E+00	.5602E+01
4	.3995E-02	.3000E-03	.3000E-03	.0000E+00	.1102E+00	.1201E+00	.1102E+00	.7470E+01
5	.4264E-02	.3750E-03	.3750E-03	.0000E+00	.1003E+00	.1126E+00	.1003E+00	.9337E+01
6	.4448E-02	.4500E-03	.4500E-03	.0000E+00	.9178E-01	.1064E+00	.9178E-01	.1120E+02
7	.4576E-02	.5250E-03	.5250E-03	.0000E+00	.8439E-01	.1012E+00	.8439E-01	.1307E+02
8	.4668E-02	.5658E-03	.6000E-03	.3418E-04	.7804E-01	.9715E-01	.7804E-01	.1409E+02
9	.4767E-02	.5778E-03	.6750E-03	.9723E-04	.7276E-01	.9435E-01	.7276E-01	.1439E+02
10	.4839E-02	.5865E-03	.7500E-03	.1635E-03	.6811E-01	.9206E-01	.6811E-01	.1460E+02
11	.4891E-02	.5928E-03	.8250E-03	.2322E-03	.6398E-01	.9013E-01	.6398E-01	.1476E+02
12	.4933E-02	.5980E-03	.9000E-03	.3020E-03	.6028E-01	.8841E-01	.6028E-01	.1489E+02
13	.4959E-02	.6011E-03	.9750E-03	.3739E-03	.5696E-01	.8697E-01	.5696E-01	.1497E+02
14	.4976E-02	.6031E-03	.1050E-02	.4469E-03	.5397E-01	.8572E-01	.5397E-01	.1502E+02
15	.4986E-02	.6043E-03	.1125E-02	.5207E-03	.5125E-01	.8459E-01	.5125E-01	.1505E+02
16	.4988E-02	.6046E-03	.1200E-02	.5954E-03	.4877E-01	.8360E-01	.4877E-01	.1505E+02
17	.4985E-02	.6043E-03	.1275E-02	.6707E-03	.4651E-01	.8272E-01	.4651E-01	.1505E+02
18	.4979E-02	.6035E-03	.1350E-02	.7465E-03	.4443E-01	.8190E-01	.4443E-01	.1503E+02
19	.4969E-02	.6023E-03	.1425E-02	.8227E-03	.4251E-01	.8116E-01	.4251E-01	.1500E+02
20	.4955E-02	.6006E-03	.1500E-02	.8994E-03	.4074E-01	.8048E-01	.4074E-01	.1496E+02

NUMBER	EG	TG C	TW C	TFLR C	QR W/CM-2	AV M-2	RFDOT KW	QFLR W/CM-2	FUEL KG/S	MA/MV
1	.3020E+00	.1461E+03	.1177E+03	.5423E+02	.5069E-01	.3889E-02	.1213E+00	.1229E+00	.7500E-04	.2971E+02
2	.3275E+00	.3177E+03	.2645E+03	.1540E+03	.2676E+00	.7922E-02	.1487E+00	.3561E+00	.1500E-03	.2046E+02
3	.3549E+00	.4579E+03	.3994E+03	.2983E+03	.7239E+00	.1129E-01	.1461E+00	.8108E+00	.2250E-03	.1605E+02
4	.3793E+00	.5851E+03	.5308E+03	.4519E+03	.1544E+01	.1271E-01	.1281E+00	.1620E+01	.3000E-03	.1332E+02
5	.4011E+00	.7018E+03	.6549E+03	.5941E+03	.2819E+01	.1229E-01	.1050E+00	.2882E+01	.3750E-03	.1137E+02
6	.4208E+00	.8067E+03	.7667E+03	.7184E+03	.4554E+01	.1112E-01	.8403E-01	.4604E+01	.4500E-03	.9083E+01
7	.4387E+00	.8999E+03	.8657E+03	.8259E+03	.6703E+01	.9890E-02	.6732E-01	.6743E+01	.5250E-03	.8717E+01
8	.4513E+00	.9427E+03	.9116E+03	.8756E+03	.8043E+01	.9947E-02	.5797E-01	.8077E+01	.6000E-03	.7760E+01
9	.4591E+00	.9482E+03	.9182E+03	.8835E+03	.8415E+01	.1099E-01	.5316E-01	.8446E+01	.6750E-03	.7062E+01
10	.4659E+00	.9506E+03	.9215E+03	.8879E+03	.8685E+01	.1210E-01	.4902E-01	.8714E+01	.7500E-03	.6452E+01
11	.4718E+00	.9507E+03	.9223E+03	.8894E+03	.8871E+01	.1328E-01	.4542E-01	.8898E+01	.8250E-03	.5928E+01
12	.4770E+00	.9496E+03	.9218E+03	.8895E+03	.9005E+01	.1450E-01	.4223E-01	.9030E+01	.9000E-03	.5481E+01
13	.4817E+00	.9466E+03	.9193E+03	.8875E+03	.9066E+01	.1580E-01	.3946E-01	.9090E+01	.9750E-03	.5086E+01
14	.4859E+00	.9426E+03	.9156E+03	.8841E+03	.9080E+01	.1719E-01	.3701E-01	.9102E+01	.1050E-02	.4739E+01
15	.4897E+00	.9378E+03	.9111E+03	.8799E+03	.9056E+01	.1864E-01	.3482E-01	.9077E+01	.1125E-02	.4432E+01
16	.4931E+00	.9321E+03	.9056E+03	.8745E+03	.8994E+01	.2020E-01	.3288E-01	.9014E+01	.1200E-02	.4157E+01
17	.4962E+00	.9258E+03	.8994E+03	.8684E+03	.8902E+01	.2185E-01	.3114E-01	.8921E+01	.1275E-02	.3910E+01
18	.4990E+00	.9189E+03	.8927E+03	.8617E+03	.8787E+01	.2359E-01	.2957E-01	.8805E+01	.1350E-02	.3688E+01
19	.5016E+00	.9116E+03	.8854E+03	.8545E+03	.8651E+01	.2545E-01	.2815E-01	.8668E+01	.1425E-02	.3487E+01
20	.5040E+00	.9039E+03	.8777E+03	.8467E+03	.8497E+01	.2743E-01	.2687E-01	.8513E+01	.1500E-02	.3304E+01

CS= 4.00 WD=.1150 KW= 5.00 0.56X 0.30 ROOM

NUMBER	AMASS KG/S	BMASS KG/S	VMASS KG/S	PYMASS KG /S	XD M	XN M	HF M	FIRE KW
1	.3125E-02	.1000E-03	.1000E-03	.0000E+00	.1561E+00	.1587E+00	.1561E+00	.2490E+01
2	.4475E-02	.2000E-03	.2000E-03	.0000E+00	.1413E+00	.1454E+00	.1413E+00	.4980E+01
3	.5460E-02	.3000E-03	.3000E-03	.0000E+00	.1268E+00	.1329E+00	.1268E+00	.7470E+01
4	.6175E-02	.4000E-03	.4000E-03	.0000E+00	.1143E+00	.1229E+00	.1143E+00	.9960E+01
5	.6705E-02	.5000E-03	.5000E-03	.0000E+00	.1037E+00	.1147E+00	.1037E+00	.1245E+02
6	.7076E-02	.6000E-03	.6000E-03	.0000E+00	.9454E-01	.1082E+00	.9454E-01	.1494E+02
7	.7341E-02	.7000E-03	.7000E-03	.0000E+00	.8672E-01	.1029E+00	.8672E-01	.1743E+02
8	.7522E-02	.8000E-03	.8000E-03	.0000E+00	.7997E-01	.9848E-01	.7997E-01	.1992E+02
9	.7642E-02	.9000E-03	.9000E-03	.0000E+00	.7410E-01	.9483E-01	.7410E-01	.2241E+02
10	.7725E-02	.9364E-03	.1000E-02	.6358E-04	.6900E-01	.9185E-01	.6900E-01	.2332E+02
11	.7835E-02	.9497E-03	.1100E-02	.1503E-03	.6471E-01	.8980E-01	.6471E-01	.2365E+02
12	.7914E-02	.9593E-03	.1200E-02	.2407E-03	.6090E-01	.8809E-01	.6090E-01	.2389E+02
13	.7969E-02	.9660E-03	.1300E-02	.3340E-03	.5748E-01	.8665E-01	.5748E-01	.2405E+02
14	.8008E-02	.9707E-03	.1400E-02	.4293E-03	.5442E-01	.8539E-01	.5442E-01	.2417E+02
15	.8039E-02	.9744E-03	.1500E-02	.5256E-03	.5164E-01	.8425E-01	.5164E-01	.2426E+02
16	.8054E-02	.9762E-03	.1600E-02	.6238E-03	.4912E-01	.8327E-01	.4912E-01	.2431E+02
17	.8059E-02	.9769E-03	.1700E-02	.7231E-03	.4682E-01	.8240E-01	.4682E-01	.2432E+02
18	.8059E-02	.9769E-03	.1800E-02	.8231E-03	.4472E-01	.8161E-01	.4472E-01	.2432E+02
19	.8054E-02	.9762E-03	.1900E-02	.9238E-03	.4279E-01	.8088E-01	.4279E-01	.2431E+02
20	.8042E-02	.9747E-03	.2000E-02	.1025E-02	.4100E-01	.8022E-01	.4100E-01	.2427E+02

NUMBER	EG	TG C	TW C	TFLR C	QR W/CM-2	AV M-2	RFDOT KW	QFLR W/CM-2	FUEL KG/S	MA/MV
1	.2845E+00	.1697E+03	.1368E+03	.6137E+02	.6379E-01	.4797E-02	.1532E+00	.1550E+00	.1000E-03	.3125E+02
2	.3148E+00	.3499E+03	.2933E+03	.1777E+03	.3245E+00	.9866E-02	.1818E+00	.4327E+00	.2000E-03	.2237E+02
3	.3431E+00	.4891E+03	.4292E+03	.3290E+03	.8398E+00	.1396E-01	.1759E+00	.9446E+00	.3000E-03	.1820E+02
4	.3678E+00	.6114E+03	.5570E+03	.4795E+03	.1716E+01	.1571E-01	.1528E+00	.1807E+01	.4000E-03	.1544E+02
5	.3893E+00	.7197E+03	.6726E+03	.6122E+03	.2987E+01	.1549E-01	.1256E+00	.3062E+01	.5000E-03	.1341E+02
6	.4083E+00	.8154E+03	.7750E+03	.7263E+03	.4636E+01	.1442E-01	.1014E+00	.4696E+01	.6000E-03	.1179E+02
7	.4255E+00	.9001E+03	.8652E+03	.8246E+03	.6618E+01	.1319E-01	.8197E-01	.6667E+01	.7000E-03	.1049E+02
8	.4411E+00	.9763E+03	.9457E+03	.9109E+03	.8904E+01	.1204E-01	.6689E-01	.8944E+01	.8000E-03	.9403E+01
9	.4554E+00	.1045E+04	.1018E+04	.9879E+03	.1146E+02	.1105E-01	.5521E-01	.1150E+02	.9000E-03	.8491E+01
10	.4646E+00	.1065E+04	.1039E+04	.1010E+04	.1249E+02	.1155E-01	.4910E-01	.1251E+02	.1000E-02	.7725E+01
11	.4708E+00	.1066E+04	.1041E+04	.1013E+04	.1281E+02	.1258E-01	.4521E-01	.1284E+02	.1100E-02	.7122E+01
12	.4762E+00	.1066E+04	.1041E+04	.1014E+04	.1304E+02	.1367E-01	.4184E-01	.1306E+02	.1200E-02	.6595E+01
13	.4810E+00	.1064E+04	.1040E+04	.1013E+04	.1318E+02	.1482E-01	.3890E-01	.1320E+02	.1300E-02	.6130E+01
14	.4853E+00	.1061E+04	.1037E+04	.1010E+04	.1326E+02	.1601E-01	.3631E-01	.1328E+02	.1400E-02	.5720E+01
15	.4891E+00	.1057E+04	.1034E+04	.1007E+04	.1330E+02	.1725E-01	.3400E-01	.1332E+02	.1500E-02	.5359E+01
16	.4926E+00	.1053E+04	.1029E+04	.1003E+04	.1328E+02	.1856E-01	.3196E-01	.1330E+02	.1600E-02	.5033E+01
17	.4957E+00	.1048E+04	.1025E+04	.9985E+03	.1323E+02	.1993E-01	.3014E-01	.1324E+02	.1700E-02	.4741E+01
18	.4986E+00	.1042E+04	.1019E+04	.9933E+03	.1314E+02	.2136E-01	.2850E-01	.1316E+02	.1800E-02	.4477E+01
19	.5012E+00	.1036E+04	.1013E+04	.9876E+03	.1303E+02	.2285E-01	.2702E-01	.1304E+02	.1900E-02	.4239E+01
20	.5036E+00	.1030E+04	.1007E+04	.9813E+03	.1288E+02	.2443E-01	.2568E-01	.1290E+02	.2000E-02	.4021E+01

CS= 4.00 WO=.1850 KW= 5.00 0.56X 0.30 ROOM

NUMBER	AMASS KG/S	BMASS KG/S	VMASS KG/S	PYMASS KG /S	XD M	XN M	HF M	FIRE KW
1	.3605E-02	.1000E-03	.1000E-03	.0000E+00	.1660E+00	.1676E+00	.1660E+00	.2490E+01
2	.5462E-02	.2000E-03	.2000E-03	.0000E+00	.1542E+00	.1564E+00	.1542E+00	.4980E+01
3	.6936E-02	.3000E-03	.3000E-03	.0000E+00	.1410E+00	.1447E+00	.1410E+00	.7470E+01
4	.8149E-02	.4000E-03	.4000E-03	.0000E+00	.1293E+00	.1347E+00	.1293E+00	.9960E+01
5	.9123E-02	.5000E-03	.5000E-03	.0000E+00	.1190E+00	.1264E+00	.1190E+00	.1245E+02
6	.9901E-02	.6000E-03	.6000E-03	.0000E+00	.1100E+00	.1194E+00	.1100E+00	.1494E+02
7	.1050E-01	.7000E-03	.7000E-03	.0000E+00	.1020E+00	.1136E+00	.1020E+00	.1743E+02
8	.1096E-01	.8000E-03	.8000E-03	.0000E+00	.9498E-01	.1087E+00	.9498E-01	.1992E+02
9	.1133E-01	.9000E-03	.9000E-03	.0000E+00	.8875E-01	.1045E+00	.8875E-01	.2241E+02
10	.1160E-01	.1000E-02	.1000E-02	.0000E+00	.8322E-01	.1010E+00	.8322E-01	.2490E+02
11	.1181E-01	.1100E-02	.1100E-02	.0000E+00	.7827E-01	.9790E-01	.7827E-01	.2739E+02
12	.1196E-01	.1200E-02	.1200E-02	.0000E+00	.7383E-01	.9532E-01	.7383E-01	.2988E+02
13	.1208E-01	.1300E-02	.1300E-02	.0000E+00	.6983E-01	.9294E-01	.6983E-01	.3237E+02
14	.1216E-01	.1400E-02	.1400E-02	.0000E+00	.6620E-01	.9086E-01	.6620E-01	.3486E+02
15	.1220E-01	.1479E-02	.1500E-02	.2081E-04	.6291E-01	.8904E-01	.6291E-01	.3683E+02
16	.1225E-01	.1485E-02	.1600E-02	.1146E-03	.5995E-01	.8750E-01	.5995E-01	.3699E+02
17	.1232E-01	.1494E-02	.1700E-02	.2065E-03	.5734E-01	.8647E-01	.5734E-01	.3719E+02
18	.1238E-01	.1501E-02	.1800E-02	.2993E-03	.5494E-01	.8549E-01	.5494E-01	.3737E+02
19	.1243E-01	.1506E-02	.1900E-02	.3939E-03	.5272E-01	.8463E-01	.5272E-01	.3750E+02
20	.1247E-01	.1511E-02	.2000E-02	.4886E-03	.5067E-01	.8379E-01	.5067E-01	.3763E+02

NUMBER	EG	TG C	TW C	TFLR C	QR W/CM-2	AV M-2	RFDOT KW	QFLR W/CM-2	FUEL KG/S	MA/MV
1	.2659E+00	.1399E+03	.1130E+03	.5022E+02	.4236E-01	.4514E-02	.1672E+00	.1419E+00	.1000E-03	.3605E+02
2	.2896E+00	.2986E+03	.2464E+03	.1311E+03	.2084E+00	.9326E-02	.2089E+00	.3328E+00	.2000E-03	.2731E+02
3	.3145E+00	.4152E+03	.3550E+03	.2398E+03	.4997E+00	.1404E-01	.2161E+00	.6284E+00	.3000E-03	.2312E+02
4	.3362E+00	.5122E+03	.4525E+03	.3536E+03	.9440E+00	.1771E-01	.2056E+00	.1066E+01	.4000E-03	.2037E+02
5	.3554E+00	.5985E+03	.5430E+03	.4612E+03	.1570E+01	.1980E-01	.1853E+00	.1680E+01	.5000E-03	.1825E+02
6	.3724E+00	.6762E+03	.6261E+03	.5581E+03	.2384E+01	.2048E-01	.1618E+00	.2480E+01	.6000E-03	.1650E+02
7	.3877E+00	.7471E+03	.7021E+03	.6447E+03	.3385E+01	.2019E-01	.1390E+00	.3467E+01	.7000E-03	.1499E+02
8	.4016E+00	.8116E+03	.7712E+03	.7217E+03	.4556E+01	.1943E-01	.1187E+00	.4626E+01	.8000E-03	.1370E+02
9	.4142E+00	.8706E+03	.8342E+03	.7909E+03	.5883E+01	.1849E-01	.1015E+00	.5943E+01	.9000E-03	.1259E+02
10	.4259E+00	.9253E+03	.8922E+03	.8537E+03	.7359E+01	.1750E-01	.8715E-01	.7411E+01	.1000E-02	.1160E+02
11	.4368E+00	.9762E+03	.9460E+03	.9113E+03	.8974E+01	.1656E-01	.7522E-01	.9018E+01	.1100E-02	.1074E+02
12	.4470E+00	.1024E+04	.9962E+03	.9647E+03	.1072E+02	.1567E-01	.6529E-01	.1076E+02	.1200E-02	.9964E+01
13	.4565E+00	.1069E+04	.1043E+04	.1014E+04	.1238E+02	.1487E-01	.5705E-01	.1261E+02	.1300E-02	.9289E+01
14	.4656E+00	.1111E+04	.1087E+04	.1060E+04	.1455E+02	.1415E-01	.5014E-01	.1458E+02	.1400E-02	.8683E+01
15	.4733E+00	.1142E+04	.1119E+04	.1094E+04	.1620E+02	.1385E-01	.4487E-01	.1622E+02	.1500E-02	.8136E+01
16	.4775E+00	.1140E+04	.1118E+04	.1093E+04	.1636E+02	.1474E-01	.4213E-01	.1638E+02	.1600E-02	.7659E+01
17	.4812E+00	.1139E+04	.1117E+04	.1093E+04	.1651E+02	.1564E-01	.3976E-01	.1653E+02	.1700E-02	.7248E+01
18	.4846E+00	.1137E+04	.1116E+04	.1092E+04	.1663E+02	.1655E-01	.3761E-01	.1666E+02	.1800E-02	.6878E+01
19	.4876E+00	.1135E+04	.1114E+04	.1090E+04	.1672E+02	.1749E-01	.3565E-01	.1674E+02	.1900E-02	.6540E+01
20	.4905E+00	.1133E+04	.1112E+04	.1088E+04	.1679E+02	.1843E-01	.3386E-01	.1681E+02	.2000E-02	.6235E+01

CS= 4.00 WD=.2850 KW= 5.00 0.56X 0.30 ROOM

NBS-114A (REV. 7-73)

U.S. DEPT. OF COMM. BIBLIOGRAPHIC DATA SHEET	1. PUBLICATION OR REPORT NO. NBSIR 78-1511	2. Gov't Accession No.	3. Recipient's Accession No.

4. TITLE AND SUBTITLE

Experimental and Theoretical Analysis of Quasi-Steady Small-Scale Enclosure Fires

5. Publication Date October 1978

6. Performing Organization Code

7. AUTHOR(S) J. G. Quintiere, B. J. McCaffrey and K. DenBraven

8. Performing Organ. Report No.

9. PERFORMING ORGANIZATION NAME AND ADDRESS

NATIONAL BUREAU OF STANDARDS
DEPARTMENT OF COMMERCE
WASHINGTON, D.C. 20234

10. Project/Task/Work Unit No. 7515676

11. Contract/Grant No.

12. Sponsoring Organization Name and Complete Address *(Street, City, State, ZIP)*

Same as No. 9

13. Type of Report & Period Covered Final

14. Sponsoring Agency Code

15. SUPPLEMENTARY NOTES

16. ABSTRACT *(A 200-word or less factual summary of most significant information. If document includes a significant bibliography or literature survey, mention it here.)* Forty-six small-scale experiments were conducted to measure the characteristics of horizontal plastic (PMMA) pool fires in an enclosure as a function of doorway width and fuel area. A 0.30 m high enclosure was instrumented to measure sample mass loss, the upper gas layer and ceiling temperatures, heat flux to the floor, and the pressure drop across the doorway. Results are reported for the maximum steady burning period; however, a few cases do not seem to have reached a steady state. For small sample sizes, a distinct fire plume could be perceived in the enclosure, while for larger sample sizes flames tended to fill the enclosure (sometimes to within 2 or 3 cm of the floor), and extended out the door opening.

The rate of mass loss is a strong function of the radiative feedback from the enclosure. However, reduced oxygen concentration in the flow entrained by the fire plume seems also to affect the mass loss rate. For the smaller doorway widths, the rate of mass loss increases almost directly with ventilation. As the width is increased, the mass loss rate instead becomes a function of sample area and radiative heat transfer. For some sample sizes, as the doorway width is increased a maximum rate of mass loss is achieved, followed by a decrease in burning rate at higher ventilation levels. The temperatures and floor heat flux also tend to follow this trend.

The data were then compared to the results of a theoretical model. Agreement between theory and data is qualitatively good. But overall, good quantitative agreement is not achieved. This lack of agreement appears consistent with inaccuracies of the flame radiation model and an incomplete description of the flame chemistry.

17. KEY WORDS *(six to twelve entries; alphabetical order; capitalize only the first letter of the first key word unless a proper name; separated by semicolons)* Burning rate; enclosure fires; experiment; mathematical models; radiation; small scale; ventilation.

18. AVAILABILITY ☐ Unlimited	19. SECURITY CLASS (THIS REPORT)	21. NO. OF PAGES
☒ For Official Distribution. Do Not Release to NTIS*	UNCLASSIFIED	
☐ Order From Sup. of Doc., U.S. Government Printing Office Washington, D.C. 20402, SD Cat. No. C13	20. SECURITY CLASS (THIS PAGE)	22. Price
☐ Order From National Technical Information Service (NTIS) Springfield, Virginia 22151	UNCLASSIFIED	

* The main text of this report will be available in a non-NBS publication. This expanded version is for limited distribution to specialists.